

# 4'-Ethynyl-2-fluoro-2'-deoxyadenosine (EFdA) Inhibits HIV-1 Reverse Transcriptase with Multiple Mechanisms\*

Received for publication, March 3, 2014, and in revised form, June 17, 2014. Published, JBC Papers in Press, June 26, 2014, DOI 10.1074/jbc.M114.562694

Eleftherios Michailidis,<sup>a,b</sup> Andrew D. Huber,<sup>a,c</sup> Emily M. Ryan,<sup>a,b</sup> Yee T. Ong,<sup>a,b</sup> Maxwell D. Leslie,<sup>a,b</sup> Kayla B. Matzek,<sup>a,b</sup> Kamalendra Singh,<sup>a,b</sup> Bruno Marchand,<sup>a,b1</sup> Ariel N. Hagedorn,<sup>a,b</sup> Karen A. Kirby,<sup>a,b</sup> Lisa C. Rohan,<sup>d,e</sup> Eiichi N. Kodama,<sup>f2</sup> Hiroaki Mitsuya,<sup>g,h2</sup> Michael A. Parniak,<sup>i</sup> and Stefan G. Sarafianos<sup>a,b,j3</sup>

From the <sup>a</sup>Christopher Bond Life Sciences Center and Departments of <sup>c</sup>Veterinary Pathobiology and <sup>i</sup>Biochemistry, University of Missouri, Columbia, Missouri 65211, <sup>b</sup>Department of Molecular Microbiology and Immunology, University of Missouri School of Medicine, Columbia, Missouri 65211, <sup>d</sup>Magee-Womens Research Institute and <sup>e</sup>Department of Pharmaceutical Sciences, School of Pharmacy, University of Pittsburgh, Pittsburgh, Pennsylvania 15213, <sup>f</sup>Division of Emerging Infectious Diseases, Tohoku University, Sendai 980-8575, Japan, <sup>g</sup>Department of Internal Medicine, Kumamoto University, Kumamoto 860-8556, Japan, <sup>h</sup>Experimental Retrovirology Section, HIV/AIDS Malignancy Branch, National Institutes of Health, Bethesda, Maryland 20892, and <sup>i</sup>Department of Microbiology and Molecular Genetics, University of Pittsburgh School of Medicine, Pittsburgh, Pennsylvania 15219

**Background:** 4'-Ethynyl-2-fluoro-2'-deoxyadenosine (EFdA) is a highly potent nucleoside analog reverse transcriptase (RT) inhibitor with a 3'-OH.

**Results:** EFdA inhibits RT as an immediate or delayed chain terminator depending on the DNA substrate sequence. RT efficiently misincorporates EFdA, producing non-extendable mismatched primers protected from excision.

**Conclusion:** EFdA blocks RT by multiple mechanisms.

**Significance:** Understanding the EFdA inhibition mechanism will help develop better antivirals.

4'-Ethynyl-2-fluoro-2'-deoxyadenosine (EFdA) is a nucleoside analog that, unlike approved anti-human immunodeficiency virus type 1 (HIV-1) nucleoside reverse transcriptase inhibitors, has a 3'-OH and exhibits remarkable potency against wild-type and drug-resistant HIVs. EFdA triphosphate (EFdA-TP) is unique among nucleoside reverse transcriptase inhibitors because it inhibits HIV-1 reverse transcriptase (RT) with multiple mechanisms. (a) EFdA-TP can block RT as a translocation-defective RT inhibitor that dramatically slows DNA synthesis, acting as a *de facto* immediate chain terminator. Although non-translocated EFdA-MP-terminated primers can be unblocked, they can be efficiently converted back to the EFdA-MP-terminated form. (b) EFdA-TP can function as a delayed chain terminator, allowing incorporation of an additional dNTP before blocking DNA synthesis. In such cases, EFdA-MP-terminated primers are protected from excision. (c) EFdA-MP can be efficiently misincorporated by RT, leading to mismatched primers that are extremely hard to extend and are also protected from excision. The context of template sequence defines the relative contribution of each mechanism and affects the affinity of

EFdA-MP for potential incorporation sites, explaining in part the lack of antagonism between EFdA and tenofovir. Changes in the type of nucleotide before EFdA-MP incorporation can alter its mechanism of inhibition from delayed chain terminator to immediate chain terminator. The versatility of EFdA in inhibiting HIV replication by multiple mechanisms may explain why resistance to EFdA is more difficult to emerge.

The enzyme reverse transcriptase (RT) of human immunodeficiency virus type 1 (HIV-1)<sup>4</sup> has been the major target of antiretrovirals that belong to two general classes referred to as nucleoside RT inhibitors (NRTIs) and non-nucleoside RT inhibitors. Currently there are eight approved NRTIs for the treatment of HIV infection, and these are almost always components of first line therapies (1–8). Once phosphorylated, NRTI triphosphates compete with the natural dNTPs for incorporation into the viral nascent DNA chain, and because they lack a 3'-OH, they inhibit further DNA polymerization by acting as chain terminators. Despite the availability of potent antivirals, HIV can escape treatment by developing drug resistance mutations. Thus, there is a need for potent drugs that block wild-type and drug-resistant HIVs.

We have shown previously that nucleoside analogs that retain the 3'-OH group and have a modification at the 4'-position of the sugar ring can inhibit HIV-1 RT very efficiently (9).

\* This work was supported, in whole or in part, by National Institutes of Health Grants R01AI076119, R01AI076119-S1, R01AI076119-02S1, R01AI099284, R01AI100890, R21AI112417, and P01GM103368 (to S. G. S.) and AI079801 (to M. A. P.). This work was also supported by Mizzou Advantage and the Ministry of Knowledge and Economy, Bilateral International Collaborative Research and Development Program, Republic of Korea. Co-authors Drs. Hiroaki Mitsuya and Eiichi N. Kodama are inventors of EFdA, and thus there is a potential conflict of interest.

<sup>1</sup> Present Address: Gilead Sciences Inc., Foster City, CA 94404.

<sup>2</sup> Co-inventors of EFdA.

<sup>3</sup> To whom correspondence should be addressed: Christopher Bond Life Sciences Center, Depts. of Molecular Microbiology and Immunology and Biochemistry, University of Missouri, Columbia, MO 65211. Tel.: 573-882-4338; Fax: 573-884-9676; E-mail: sarafianos@missouri.edu.

<sup>4</sup> The abbreviations used are: HIV-1, human immunodeficiency virus type 1; NRTI, nucleoside RT inhibitor; EFdA, 4'-ethynyl-2-fluoro-2'-deoxyadenosine; TFV, tenofovir; MP, monophosphate; DP, diphosphate; TP, triphosphate; T/P, template/primer; ICT, immediate chain terminator; DCT, delayed chain terminator; SPR, surface plasmon resonance; N-site, nucleotide-binding or pre-translocation site; P-site, primer-binding or post-translocation site.

## Multiple Mechanisms of RT Inhibition by EFdA

We also reported that 4'-ethynyl-2-fluoro-2'-deoxyadenosine (EFdA) is a deoxyadenosine analog with anti-HIV efficacy at subnanomolar concentrations in primary cells, making it the most potent NRTI described to date (10–13). Unlike all approved anti-HIV NRTIs, EFdA possesses a 3'-OH, which mimics the structure of normal dNTPs (see Fig. 1A). It has been demonstrated that this property provides enhanced phosphorylation of the NRTIs by cellular kinases increasing their antiviral efficacy (14). In addition, EFdA has 4'-ethynyl and 2-fluoro substitutions, which also contribute to its extraordinary selectivity index of about 200,000 as determined after initial antiviral characterization of a series of 4'-substituted analogs (9, 11). We have shown that EFdA is resistant to degradation by adenosine deaminase, providing an enhanced half-life to the compound compared with other NRTIs (11, 15). EFdA is very effective not only against wild-type HIV but also against drug-resistant strains and has displayed synergistic antiviral effects when combined with other inhibitors such as the recently approved second generation non-NRTI rilpivirine (16). We have also shown that EFdA is significantly better than tenofovir (TFV), zidovudine, and emtricitabine in blocking simian immunodeficiency virus replication in monkey peripheral blood mononuclear cells and that it was highly effective at treating simian immunodeficiency virus infection and AIDS symptoms in simian immunodeficiency virus-infected macaques with advanced AIDS with no apparent signs of toxicity (17).

Here we used a series of biochemical experiments and demonstrated that EFdA triphosphate (EFdA-TP) blocks RT with multiple mechanisms. Specifically, we found that, unlike approved anti-HIV NRTIs, EFdA-TP can act as a *de facto* immediate or delayed chain terminator in a manner that depends on the sequence of the nucleic acid template. Moreover, EFdA monophosphate (EFdA-MP) is misincorporated by RT, resulting in mismatched primers that are very difficult to extend. Finally, the detailed analysis of the versatile mechanisms of RT inhibition by EFdA provides novel insights into a reduced resistance profile for EFdA because delayed termination seems to protect EFdA-MP-terminated primers from excision.

## EXPERIMENTAL PROCEDURES

### Enzymes, Nucleic Acids, Nucleotides, and Nucleotide Analogs

HIV-1 RT was expressed and purified as described previously (10, 18–23). RT was expressed in JM-109 cells (Invitrogen) and purified by nickel affinity chromatography and Mono Q anion exchange chromatography (24). Oligonucleotides used in this study were chemically synthesized and purchased from Integrated DNA Technologies (Coralville, IA). Sequences of the DNA substrates are shown in Table 1. Deoxynucleotide triphosphates and dideoxynucleotide triphosphates were purchased from Fermentas (Glen Burnie, MD). Concentrations of nucleotides were calculated spectrophotometrically on the basis of absorption at 260 nm and their extinction coefficients. All nucleotides were treated with inorganic pyrophosphatase (Roche Diagnostics) as described previously (25) to remove traces of PP<sub>i</sub> contamination that might interfere with the rescue assay.

### Active Site Titration of HIV-1 RT

To determine polymerization-competent RT populations used in this study, we first carried out active site titration assays using pre-steady state experiments (26, 27). A fixed concentration of RT (50 nM; determined by absorbance measurements) in RT buffer (50 mM NaCl and 50 mM Tris-HCl, pH 7.8) was incubated with increasing concentrations of template/primer (T/P; T<sub>d31</sub>/P<sub>d18</sub> where T<sub>d31</sub> is the DNA template of 31 nucleotides in length annealed to P<sub>d18</sub>, which is a DNA primer of 18 nucleotides in length) followed by rapidly mixing with a solution containing 5 mM MgCl<sub>2</sub> and 50 μM dATP in the same RT buffer using a rapid quench-flow instrument (RQF-3, KinTek Corp., Austin, TX) at 37 °C for 0.005–1 s. The reactions were quenched by the addition of 150 mM EDTA. The products were resolved on 15% polyacrylamide and 7 M urea gels. In this and in subsequent assays, the gels were scanned with a Typhoon FLA 9000 phosphorimaging system (GE Healthcare), and densitometry analysis was performed using ImageQuant TL software (GE Healthcare). The amounts of extended primer (P) were plotted against time, and the data were fit to a biphasic equation (Equation 1) using GraphPad Prism 4.0 (GraphPad Software Inc., La Jolla, CA) (26),

$$P = A(1 - e^{-k_{\text{obs}}t}) + k_{\text{ss}}t \quad (\text{Eq. 1})$$

where *A* is the amplitude of the burst phase that represents the E-DNA complex at the start of the reaction, *k*<sub>obs</sub> is the observed burst rate constant for dNTP incorporation, *k*<sub>ss</sub> corresponds to the steady state rate constant, and *t* is the reaction time. Next, the active site concentration and T/P dissociation constant (*K*<sub>d(DNA)</sub>) were determined by plotting the amplitude (*A*) against T/P concentration. The data were fit by non-linear regression to a quadratic equation,

$$A = 0.5((K_{d(\text{DNA})} + [\text{RT}] + [\text{DNA}]) - \sqrt{0.25(K_{d(\text{DNA})} + [\text{RT}] + [\text{DNA}])^2 - ([\text{RT}][\text{DNA}])}) \quad (\text{Eq. 2})$$

where [RT] is the concentration of actively binding polymerase molecules. Subsequent pre-steady state experiments were performed using corrected active site concentrations.

### Gel-based Drug Susceptibility Assays: Inhibition of HIV-1 RT-catalyzed DNA Synthesis by EFdA-TP and ddATP

DNA template was annealed to 5'-Cy3-labeled DNA primer at a 3:1 molar ratio. For these experiments, we used T<sub>d31</sub>/P<sub>d18</sub> and T<sub>d26</sub>/P<sub>d18+5</sub> where P<sub>d18+5</sub> is an 18-mer DNA primer shifted by five nucleotides relative to the P<sub>d18</sub> primer. Throughout most of our work, we carried out our analyses using two types of primers (in this case, P<sub>d18</sub> and P<sub>d18+5</sub>) that allowed us to interrogate two different template sites where RT incorporates dAMP or EFdA-MP at different affinities and different translocation efficiencies. To monitor primer extension, the DNA/DNA hybrid (20 nM) was incubated at 37 °C with RT (20 nM) in RT buffer. Varying amounts of EFdA-TP or ddATP were added, and the reactions were initiated by the addition of 6 mM MgCl<sub>2</sub> in a final volume of 20 μl. All dNTPs were present at a final concentration of 10 μM. The reactions were terminated after 15 min by adding an equal volume of 100% formamide containing

traces of bromophenol blue. The products were resolved on a 15% polyacrylamide and 7 M urea gel and analyzed as described before (10, 22, 23).

### Effect of Template Sequence on RT Inhibition by EFdA-TP

Various T/Ps (oligonucleotide sequences are shown in Table 1) were used to determine the effect of the DNA sequence on the mechanism of inhibition by EFdA-TP. The experiments were carried out as described above.

### Surface Plasmon Resonance Assays

Surface plasmon resonance (SPR) was used to determine the kinetic constants of nucleotide triphosphate or EFdA-TP binding to HIV-1 RT. To allow nucleotide binding to the reverse transcriptase, the enzyme was covalently cross-linked to a double-stranded DNA/DNA T/P as described before (24). Briefly, a thiol-modified DNA primer at the N<sup>2</sup> position of a guanosine residue (indicated by X in 5'-ACAGTCCCTGTTCCGXC-GCG-3') was heat-annealed to a 5'-biotinylated DNA template (5'-biotin-TAGATCAGTCATGCTCCGCGCCCGAACAGGG-ACTGTG) at a 3:1 T/P ratio (Table 1). The double-stranded DNA was cross-linked to RT containing mutation Q258C by incubating overnight at 30 °C in a mixture containing 25 mM Tris, pH 7.8, 75 mM NaCl, 10 mM MgCl<sub>2</sub>, and 100 μM ddGTP. The incorporation of the dideoxynucleotide into the T/P (DNA<sub>ddGMP</sub>) aligns the thiol-modified G with the cysteine 258 of RT and allows disulfide bond formation as we have previously described (24). The covalent RT-DNA<sub>ddGMP</sub> complex was purified by tandem nickel affinity/ion exchange chromatography to remove unreacted DNA and enzyme (28). The purified complex was immobilized on a streptavidin sensor chip on a Biacore T100 system (GE Healthcare). RT-DNA<sub>ddGMP</sub> was flowed over the chip surface of channel 2 until ~8,000 response units were immobilized through the very strong interactions of the biotinylated RT-DNA<sub>ddGMP</sub> with the streptavidin sensor chip. Channel 1 was left untouched and was later used as a control surface. Increasing concentrations of dATP (1–1,000 nM) or EFdA-TP (5–1,000 nM) were flowed in channels 1 and 2 in RT buffer and 10 mM MgCl<sub>2</sub> for 2 min to allow nucleotide association and dissociation. The signal observed in channel 1 (control channel) was subtracted from the signal obtained from the RT-DNA<sub>ddGMP</sub> channel 2. The ddGTP at the 3'-end of the DNA primer prevents incorporation of the dATP or EFdA-TP and allows estimation of their dissociation and association rates, the ratio of which provides the  $K_d$  equilibrium binding constant of the binding of the incoming nucleotide triphosphate to the RT-DNA<sub>ddGMP</sub> complex. Optimal analysis of the binding signal was performed using a two-state reaction protocol that assumes a conformational change associated with substrate binding in the Biacore T100 software to obtain measured kinetic constants. Specifically, the overall equilibrium dissociation constant  $K_d$  for this type of two-state reaction protocol is defined by  $(k_{d1}/k_{a1}) \cdot (k_{d2}/(k_{d2} + k_{a2}))$  where  $k_{a1}$  is the association rate constant for substrate binding,  $k_{d1}$  is the dissociation rate constant for substrate from the complex,  $k_{a2}$  is the forward rate constant for the conformational change, and  $k_{d2}$  is the reverse rate constant for the conformational change.

### Pre-steady State Kinetics of dATP and EFdA-TP Incorporation

Pre-steady state kinetics analysis was performed using dATP or EFdA-TP single nucleotide incorporation experiments catalyzed by RT. The optimal rate of polymerization ( $k_{pol}$ ) was determined using the rapid quench-flow method as described before (19, 26, 27, 29). Specifically, a solution containing 50 nM RT and 50 nM T<sub>d31</sub>/P<sub>d18</sub> or T<sub>d26</sub>/P<sub>d18+5</sub> in RT buffer was rapidly mixed with a solution of 5 mM MgCl<sub>2</sub> and 1–50 μM dATP or EFdA-TP for reaction times ranging between 0.005 and 2 s followed by quenching with 150 mM EDTA. The reaction products were resolved and quantified as described above. The observed burst rates ( $k_{obs}$ ) at each dATP or EFdA-TP concentration were determined by fitting the data to Equation 1 and solving the equation by non-linear regression using GraphPad Prism 4.0.

To determine the optimal rates of dATP and EFdA-TP incorporation ( $k_{pol}$ ) and their binding to the enzyme-DNA complex ( $K_{d(dATP)}$  or  $K_{d(EFdA-TP)}$ ), observed burst rates ( $k_{obs}$ ) were fit to the following hyperbolic equation.

$$k_{obs} = (k_{pol}[\text{dNTP}]) / (K_{d(\text{dNTP})} + [\text{dNTP}]) \quad (\text{Eq. 3})$$

All experiments were carried out independently at least two times, and the standard deviations of the kinetic parameters are reported in the respective tables.

### Pre-steady State Kinetics of dATP and EFdA-TP Misincorporation

We used pre-steady state kinetics to monitor the misincorporation of dAMP and EFdA-MP opposite an A template base using the T<sub>d31(1A)</sub>/P<sub>d18</sub> or T<sub>d31(6A)</sub>/P<sub>d18+5</sub> template/primer, which has an A at the first template overhang position when P<sub>d18</sub> or P<sub>d18+5</sub> was used as the primer, respectively (DNA sequences are shown in Table 1). We used both P<sub>d18</sub> and P<sub>d18+5</sub> primers to interrogate potential differences in misincorporation efficiency at two template sites where substrates are incorporated at different efficiencies. Similarly, we monitored misincorporation of dATP and EFdA-TP opposite G using T<sub>d31(1G)</sub>/P<sub>d18</sub> or T<sub>d31(6G)</sub>/P<sub>d18+5</sub> and misincorporation opposite a C using T<sub>d31(1C)</sub>/P<sub>d18</sub> or T<sub>d31(6C)</sub>/P<sub>d18+5</sub>. In these experiments, a solution containing 30 nM RT and a 20 nM concentration of the corresponding T/P in RT buffer was mixed with a solution of 6 mM MgCl<sub>2</sub> and various concentrations of dATP or EFdA-TP for the indicated reaction times followed by quenching with an equal volume of formamide. The reaction products were resolved and quantified as described above. Further analysis was carried out as described for the match pre-steady state kinetics experiments.

### Site-specific Fe<sup>2+</sup> Footprinting Assays

Site-specific Fe<sup>2+</sup> footprints were monitored on 5'-Cy3-labeled DNA templates. 100 nM 5'-Cy3-T<sub>d43</sub>/P<sub>d30</sub> or 5'-Cy3-T<sub>d43</sub>/P<sub>d30+5</sub> was incubated with 600 nM RT in a buffer containing 120 mM sodium cacodylate, pH 7.0, 20 mM NaCl, 6 mM MgCl<sub>2</sub>, and 1 μM EFdA-TP or 5 μM ddATP to allow quantitative chain termination. Prior to treatment with Fe<sup>2+</sup>, complexes were preincubated for 7 min with increasing concentrations of the next incoming nucleotide (dTTP). The complexes were treated with ammonium iron sulfate (1 mM) as



## Multiple Mechanisms of RT Inhibition by EFdA

described previously (10, 30). This reaction relies on autooxidation of  $\text{Fe}^{2+}$  (31) to create a local concentration of hydroxyl radicals that cleave the DNA at the nucleotide closest to the  $\text{Fe}^{2+}$  specifically bound to the RNase H active site. The two types of T/P systems carrying  $\text{P}_{\text{d18}}$  and  $\text{P}_{\text{d18+5}}$  primers allowed us to interrogate the translocation efficiencies in different nucleic acid sequence contexts.

### Extension of EFdA-MP-terminated Primers

$\text{T}_{\text{d31}}/\text{P}_{\text{d18-EFdA-MP}}$  (chemically prepared T/P possessing EFdA-MP at the 3'-end of the primer) and  $\text{T}_{\text{d26}}/\text{P}_{\text{d18+5-EFdA-MP}}$  were prepared by incubating 1  $\mu\text{M}$  EFdA-TP, a 1  $\mu\text{M}$  concentration of the corresponding T/P, 1  $\mu\text{M}$  RT, and 6 mM  $\text{MgCl}_2$  in RT buffer. The reactions were carried out at 37 °C for 1 h. Similarly, for the extension of the mismatched primers,  $\text{T}_{\text{d31(6C)}}/\text{P}_{\text{d18+5-EFdA-MP}}$ ,  $\text{T}_{\text{d31(6G)}}/\text{P}_{\text{d18+5-EFdA-MP}}$ , and  $\text{T}_{\text{d31(6A)}}/\text{P}_{\text{d18+5-EFdA-MP}}$  were prepared by incubating 20  $\mu\text{M}$  EFdA-TP, a 1  $\mu\text{M}$  concentration of the corresponding T/P, 2  $\mu\text{M}$  RT, and 6 mM  $\text{MgCl}_2$  in RT buffer. The reactions were carried out at 37 °C for 4 h. After incorporation of EFdA-MP, the various T/ $\text{P}_{\text{EFdA-MP}}$  substrates were purified using the QIAquick nucleotide removal kit (Qiagen, Valencia, CA). Under these conditions, the extension of T/P to T/ $\text{P}_{\text{EFdA-MP}}$  was complete. Purified  $\text{T}_{\text{d31}}/\text{P}_{\text{d18-EFdA-MP}}$ ,  $\text{T}_{\text{d26}}/\text{P}_{\text{d18+5-EFdA-MP}}$ ,  $\text{T}_{\text{d31(6C)}}/\text{P}_{\text{d18+5-EFdA-MP}}$ ,  $\text{T}_{\text{d31(6G)}}/\text{P}_{\text{d18+5-EFdA-MP}}$ , or  $\text{T}_{\text{d31(6A)}}/\text{P}_{\text{d18+5-EFdA-MP}}$  (5 nM) was incubated with 20 nM RT in RT buffer and 6 mM  $\text{MgCl}_2$ . The first incoming nucleotide was added at different concentrations (0–50  $\mu\text{M}$ ) in the presence of the other dNTPs (1  $\mu\text{M}$ ). The reactions were incubated at 37 °C for 5 and 30 min, and products were analyzed as described above.

### Pre-steady State Kinetics of dTTP Incorporation to T/ $\text{P}_{\text{EFdA-MP}}$

Pre-steady state kinetics analysis of dTTP incorporation to T/ $\text{P}_{\text{EFdA-MP}}$  was performed using  $\text{T}_{\text{d31}}/\text{P}_{\text{d18-EFdA-MP}}$ ,  $\text{T}_{\text{d26}}/\text{P}_{\text{d18+5-EFdA-MP}}$ , or  $\text{T}_{\text{d26(5C)}}/\text{P}_{\text{d18+5(5G)-EFdA-MP}}$ . In these experiments, a solution containing 30 nM RT and a 20 nM concentration of the corresponding T/P in RT buffer was mixed with a solution of 6 mM  $\text{MgCl}_2$  and various concentrations of dTTP for 30 s to 10 min followed by quenching with an equal volume of formamide. The reaction products were resolved and quantified as described above. Further analysis was carried out as described for the match pre-steady state kinetics experiments.

### $\text{PP}_i$ - and ATP-dependent Excision and Rescue of T/ $\text{P}_{\text{EFdA-MP}}$

*$\text{PP}_i$ -dependent Excision of T/ $\text{P}_{\text{EFdA-MP}}$* — $\text{T}_{\text{d26}}/\text{P}_{\text{d18+5-EFdA-MP-dTMP}}$  was prepared similarly to  $\text{T}_{\text{d26}}/\text{P}_{\text{d18+5-EFdA-MP}}$ . After EFdA-MP incorporation, 100  $\mu\text{M}$  dTTP was added to the reaction and incubated at 37 °C for an additional 1 h. The purification of the terminated primer was performed as described before. 20 nM purified  $\text{T}_{\text{d31}}/\text{P}_{\text{d18-EFdA-MP}}$  or  $\text{T}_{\text{d26}}/\text{P}_{\text{d18+5-EFdA-MP-dTMP}}$  was incubated at 37 °C with 60 nM RT in the presence of 150  $\mu\text{M}$   $\text{PP}_i$  in RT buffer and 6 mM  $\text{MgCl}_2$ . Aliquots of the reaction were stopped at different times (0–30 min) and analyzed as described above.

*ATP-dependent Rescue of T/ $\text{P}_{\text{EFdA-MP}}$* —20 nM purified  $\text{T}_{\text{d31}}/\text{P}_{\text{d18-EFdA-MP}}$  was incubated with 60 nM RT in the presence of 3.5 mM ATP, 100  $\mu\text{M}$  dATP, 0.5  $\mu\text{M}$  dTTP, and 10  $\mu\text{M}$  ddGTP in RT buffer and 10 mM  $\text{MgCl}_2$ . Similarly, 20 nM purified  $\text{T}_{\text{d26}}/$

$\text{P}_{\text{d18+5-EFdA-MP-dTMP}}$  was incubated with 60 nM RT in the presence of 3.5 mM ATP, 100  $\mu\text{M}$  dTTP, and 10  $\mu\text{M}$  ddCTP in RT buffer and 10 mM  $\text{MgCl}_2$ . Reactions were arrested at various time points (0–90 min) and analyzed as described above. Control reactions without dNTPs and ATP (no excision; no incorporation) or without ATP (no excision; incorporation) were incubated for the maximum time (90 min).

*$\text{PP}_i$ -dependent Excision of T/ $\text{P}_{\text{EFdA-MP}}$  in Which EFdA-MP Is Incorporated as a Match or Mismatch*—20 nM purified  $\text{T}_{\text{d31(6X)}}/\text{P}_{\text{d18+5-EFdA-MP}}$  (where X = T, A, C, or G) was incubated at 37 °C with 60 nM RT in the presence of 150  $\mu\text{M}$   $\text{PP}_i$  in RT buffer and 6 mM  $\text{MgCl}_2$ . Aliquots of the reaction were stopped at different times (0–20 min) and analyzed as described above.

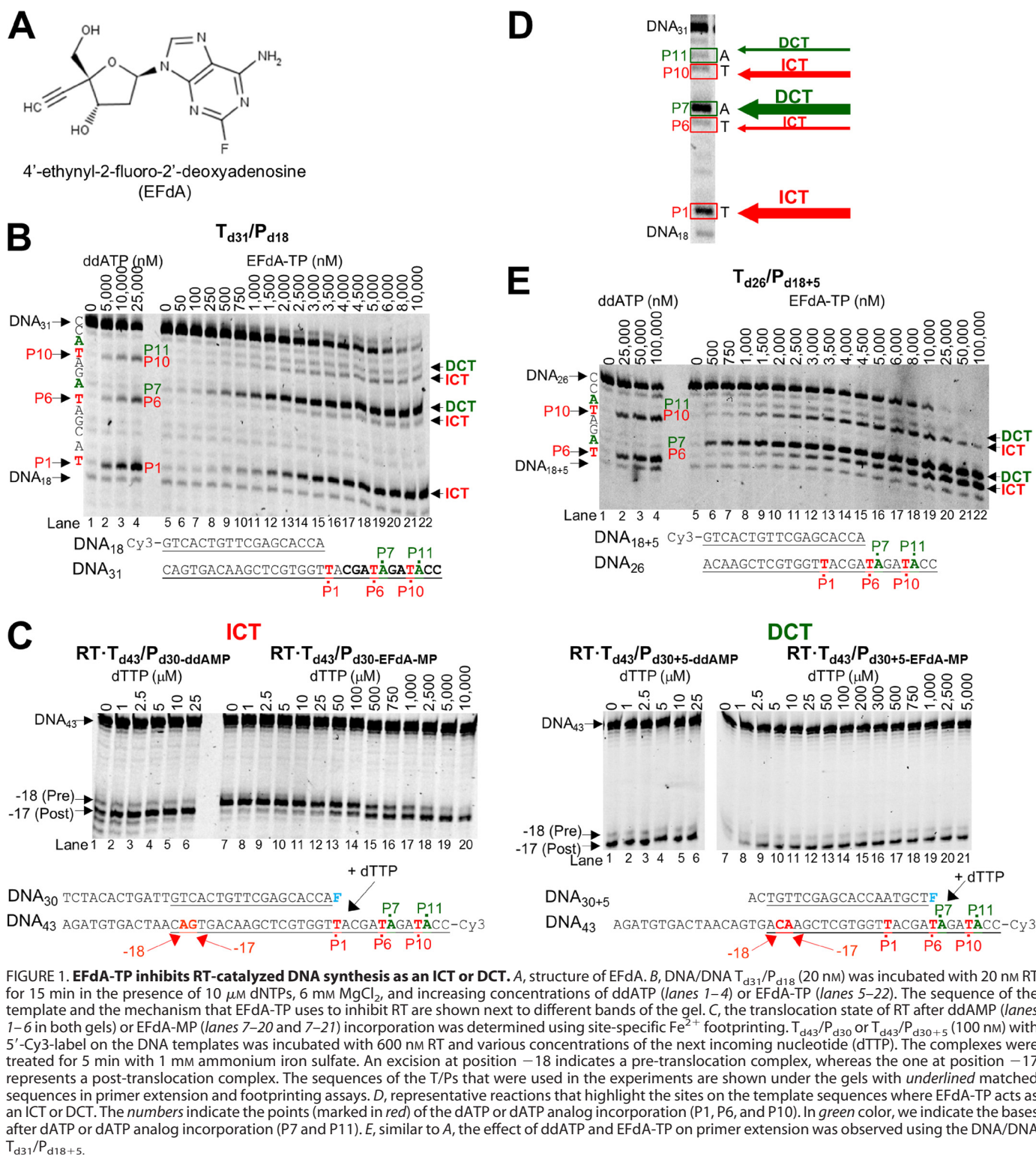
### EFdA and Tenofovir Combination Studies: Inhibition of HIV-1 RT-catalyzed DNA Synthesis and Stopping Patterns by EFdA-TP and TFV-DP

We monitored primer extension using two T/P systems. (a) A shorter T/P,  $\text{T}_{\text{d31(7C)}}/\text{P}_{\text{d18}}$  (20 nM), was incubated at 37 °C with RT (20 nM) in RT buffer. Varying amounts of EFdA-TP (0–8  $\mu\text{M}$ ) and tenofovir diphosphate (TFV-DP; 0–2  $\mu\text{M}$ ) were added, and the reactions were initiated by the addition of 6 mM  $\text{MgCl}_2$  in a final volume of 20  $\mu\text{l}$ . All dNTPs were present at a final concentration of 1  $\mu\text{M}$ . The reactions were terminated after 15 min by adding an equal volume of 100% formamide containing traces of bromophenol blue. The products were analyzed as described above. (b) Using a longer template, we compared the stopping patterns of EFdA-TP and TFV-DP. Specifically,  $\text{T}_{\text{d100}}/\text{P}_{\text{d18(100)}}$  (50 nM) was incubated at 37 °C with RT (20 nM) in RT buffer, 6 mM  $\text{MgCl}_2$ , 1  $\mu\text{M}$  dNTPs, and 240 nM EFdA-TP or 2  $\mu\text{M}$  TFV-DP. The reactions were terminated after 15 min by adding an equal volume of 100% formamide containing traces of bromophenol blue, and the products were analyzed as described above.

## RESULTS

*EFdA-TP Inhibits RT with Multiple Mechanisms: EFdA-TP Inhibits RT Primarily as an Effective Immediate or Delayed Chain Terminator (ICT or DCT)*—All NRTIs approved for the treatment of HIV infection mimic the natural dNTPs, but because they lack a 3'-OH group, once incorporated into the nascent DNA they act as immediate (or obligate) chain terminators. Primer extension assays show that despite having a 3'-OH EFdA-TP inhibits RT-catalyzed DNA synthesis mainly at the point of incorporation as a *de facto* ICT, similar to other ICTs such as ddATP (Fig. 1B; strong stops at positions of incorporation P1 and to a lesser extent at P10). For the sake of simplicity, we use the term “immediate chain terminator” in lieu of the more accurate “*de facto* immediate chain terminator” as EFdA-TP causes a dramatic but not 100% complete suppression of primer extension (eventually some primer extension can be observed at high dNTP concentrations).

However, our data show that EFdA-TP can also inhibit RT as a DCT. Specifically, our primer extension assays revealed additional bands that do not correspond to positions where EFdA-TP or other dATP analogs are expected to be incorporated. Hence, there are strong bands at positions P7 and to a



**FIGURE 1. EFdA-TP inhibits RT-catalyzed DNA synthesis as an ICT or DCT.** *A*, structure of EFdA. *B*, DNA/DNA<sub>31</sub>/P<sub>d18</sub> (20 nM) was incubated with 20 nM RT for 15 min in the presence of 10 μM dNTPs, 6 mM MgCl<sub>2</sub>, and increasing concentrations of ddATP (lanes 1–4) or EFdA-TP (lanes 5–22). The sequence of the template and the mechanism that EFdA-TP uses to inhibit RT are shown next to different bands of the gel. *C*, the translocation state of RT after ddAMP (lanes 1–6 in both gels) or EFdA-MP (lanes 7–20 and 7–21) incorporation was determined using site-specific Fe<sup>2+</sup> footprinting. T<sub>d43</sub>/P<sub>d30</sub> or T<sub>d43</sub>/P<sub>d30+5</sub> (100 nM) with 5'-Cy3-label on the DNA templates was incubated with 600 nM RT and various concentrations of the next incoming nucleotide (dTTP). The complexes were treated for 5 min with 1 mM ammonium iron sulfate. An excision at position –18 indicates a pre-translocation complex, whereas the one at position –17 represents a post-translocation complex. The sequences of the T/Ps that were used in the experiments are shown under the gels with underlined matched sequences in primer extension and footprinting assays. *D*, representative reactions that highlight the sites on the template sequences where EFdA-TP acts as an ICT or DCT. The numbers indicate the points (marked in red) of the dATP or dATP analog incorporation (P1, P6, and P10). In green color, we indicate the bases after dATP or dATP analog incorporation (P7 and P11). *E*, similar to *A*, the effect of ddATP and EFdA-TP on primer extension was observed using the DNA/DNA<sub>31</sub>/P<sub>d18+5</sub>.

less extent at P11, suggesting that EFdA-TP can act as a DCT primarily when incorporated at P6 and to a lesser extent at P10. In these cases after RT incorporates EFdA-MP at the P6 and P10 positions, it continues incorporating the next dNTP before DNA synthesis is stalled. We confirmed these findings using an oligonucleotide substrate with a shorter template but longer primer sequence that allowed examination of EFdA-MP incorporation only at the P6 and P10 sites (T<sub>d26</sub>/P<sub>d18+5</sub>; Fig. 1E).

Hence, EFdA-TP acts exclusively as an ICT at P1 and mostly as an ICT at P10, whereas it acts primarily as a DCT at P6 and to a lesser extent at P10 (Fig. 1, B and E). Using hydroxyl radical footprinting assays of RT bound to an EFdA-MP-terminated T/P (T/P<sub>EFdA-MP</sub>) we demonstrated a correlation of ICT inhibition (such as at P1 site) and a decreased translocation of RT from the nucleotide-binding or pre-translocation site (N-site; cleavage at –18) to the primer-binding or post-translocation

# Multiple Mechanisms of RT Inhibition by EFdA

**TABLE 1**

## DNA oligonucleotide sequences used in this study

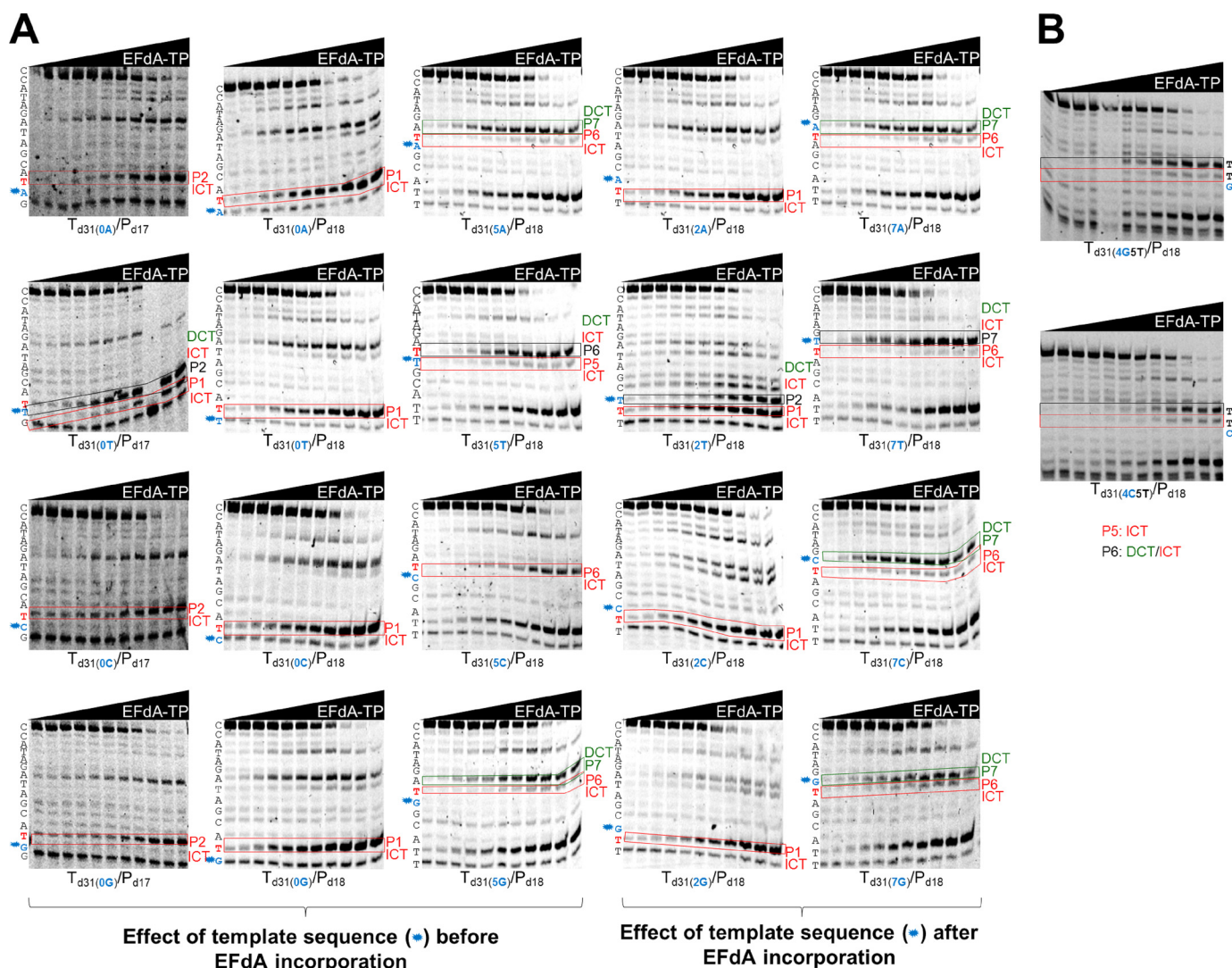
An example of the oligonucleotide abbreviation is as follows: T<sub>d31(2T)</sub>/P<sub>d18</sub>, template DNA of 31 nucleotides in length with a T in the second unpaired position after annealing to the corresponding 18-mer DNA primer. The bases that vary in similar sequences are marked in red. P<sub>d18+5</sub> is a primer that is annealed on a template five nucleotides further than P<sub>d18</sub>. In each group of templates, the varying base is indicated inside parentheses: T<sub>d31(6G)</sub>. For the SPR experiments, a thiol-modified DNA primer containing a disulfide on the N<sup>2</sup> of a guanosine residue is indicated by X in the sequence. Cy3 or biotin labels are indicated next to the sequences.

Polymerization assays	
<b>T<sub>d100</sub></b>	5' TAG TGT GTG CCC GTC TGT TGT GTG ACT CTG GTA ACT AGA GAT CCC TCA GAC CCT TTT AGT CAG TGT GGA AAA TCT CTA GCA GTG GCG CCC GAA CAG GGA C
<b>P<sub>d18(100)</sub></b>	5' GTC CCT GTT CGG GCG CCA
<b>T<sub>d31</sub> [=T<sub>d31(0T/2A/5A/6T/7A)</sub>]</b>	5' CCA TAG ATA GCA TTG GTG CTC GAA CAG TGA C
<b>P<sub>d18</sub></b>	5' Cy3 GTC ACT GTT CGA GCA CCA
<b>T<sub>d31(0A)</sub></b>	5' CCA TAG ATA GCA TAG GTG CTC GAA CAG TGA C
<b>T<sub>d31(0C)</sub></b>	5' CCA TAG ATA GCA TCG GTG CTC GAA CAG TGA C
<b>T<sub>d31(0G)</sub></b>	5' CCA TAG ATA GCA TGG GTG CTC GAA CAG TGA C
<b>P<sub>d18(0T)</sub></b>	5' Cy3 GTC ACT GTT CGA GCA CCT
<b>P<sub>d18(0G)</sub></b>	5' Cy3 GTC ACT GTT CGA GCA CCG
<b>P<sub>d18(0C)</sub></b>	5' Cy3 GTC ACT GTT CGA GCA CCC
<b>P<sub>d17</sub></b>	5' Cy3 GTC ACT GTT CGA GCA CC
<b>T<sub>d31(2T)</sub></b>	5' CCA TAG ATA GCT TTG GTG CTC GAA CAG TGA C
<b>T<sub>d31(2C)</sub></b>	5' CCA TAG ATA GCC TTG GTG CTC GAA CAG TGA C
<b>T<sub>d31(2G)</sub></b>	5' CCA TAG ATA GCG TTG GTG CTC GAA CAG TGA C
<b>T<sub>d31(7T)</sub></b>	5' CCA TAG TTA GCG TTG GTG CTC GAA CAG TGA C
<b>T<sub>d31(7C)</sub></b>	5' CCA TAG CTA GCG TTG GTG CTC GAA CAG TGA C
<b>T<sub>d31(7G)</sub></b>	5' CCA TAG GTA GCG TTG GTG CTC GAA CAG TGA C
<b>T<sub>d31(5T)</sub> [=T<sub>d31(4G5T)</sub>]</b>	5' CCA TAG ATT GCA TTG GTG CTC GAA CAG TGA C
<b>T<sub>d31(4C5T)</sub></b>	5' CCA TAG ATT CCA TTG GTG CTC GAA CAG TGA C
<b>T<sub>d31(5C)</sub></b>	5' CCA TAG ATC GCA TTG GTG CTC GAA CAG TGA C
<b>T<sub>d31(5G)</sub></b>	5' CCA TAG ATG GCA TTG GTG CTC GAA CAG TGA C
<b>T<sub>d31(1A)</sub></b>	5' CCA TAG ATA GCA ATG GTG CTC GAA CAG TGA C
<b>T<sub>d31(1C)</sub></b>	5' CCA TAG ATA GCA CTG GTG CTC GAA CAG TGA C
<b>T<sub>d31(1G)</sub></b>	5' CCA TAG ATA GCA GTG GTG CTC GAA CAG TGA C
<b>T<sub>d31(6A)</sub></b>	5' CCA TAG AAA GCA GTG GTG CTC GAA CAG TGA C
<b>T<sub>d31(6C)</sub></b>	5' CCA TAG ACA GCA GTG GTG CTC GAA CAG TGA C
<b>T<sub>d31(6G)</sub></b>	5' CCA TAG AGA GCA GTG GTG CTC GAA CAG TGA C
<b>T<sub>d26</sub></b>	5' CCA TAG ATA GCA TTG GTG CTC GAA CA
<b>P<sub>d18+5</sub></b>	5' Cy3 TGT TCG AGC ACC AAT GCT
<b>T<sub>d26</sub> (5C)</b>	5' CCA TAG ATC GCA TTG GTG CTC GAA CA
<b>P<sub>d18+5</sub> (5G)</b>	5' Cy3 TGT TCG AGC ACC AAT GCG
Surface Plasmon Resonance	
<b>T<sub>d20</sub></b>	5' ACA GTC CCT GTT CGG XCG CG
<b>P<sub>d37</sub></b>	5' biotin TAG ATC AGT CATGCTCCGCGCCCCGAACAGGGACTGTG
Footprinting assays	
<b>T<sub>d43</sub></b>	5' Cy3 CCA TAG ATA GCA TTG GTG CTC GAA CAG TGA CAA TCA GTG TAG A
<b>P<sub>d30</sub></b>	5' TCT ACA CTG ATT GTC ACT GTT CGA GCA CCA
<b>P<sub>d30+5</sub></b>	5' ACT GTT CGA GCA CCA ATG CT

site (P-site; cleavage at −17) (Fig. 1C). Therefore, when EFdA-TP inhibits RT as an ICT it acts as a translocation-defective RT inhibitor. In turn, footprinting assays at sites where EFdA acts as a DCT (such as P6) demonstrated that T/P<sub>EFdA-MP</sub>

is translocated to the P-site (Fig. 1C). Collectively, these experiments show that EFdA-TP can act both as an ICT and as a DCT depending on the template sequence and how it allows translocation of RT on T/P<sub>EFdA-MP</sub> (Figs. 1, 8, and 9).





**FIGURE 2. Effect of template sequence on mechanism of inhibition by EFdA-TP.** Primer extension assays were performed by incubating various DNA/DNA T/Ps with 20 nM RT for 15 min in the presence of 10  $\mu$ M dNTPs, 6 mM MgCl<sub>2</sub>, and increasing concentrations of EFdA-TP. The sequence of the template is shown next to the gels. Twenty templates with A, T, C, or G at the P0, P2, P5, and P7 positions were used. The nucleotides that vary are shown in blue color and indicated with an asterisk next to the gel bands. In red color, we highlight the T positions where EFdA-TP is expected to be incorporated. Immediate and delayed chain terminations are shown in red and green boxes, respectively. Blue color and asterisks highlight the positions of the nucleotides that vary among different gels.

*The Mechanism of RT Inhibition by EFdA-TP Is Sequence-dependent*—To further explore the effect of the T/P sequence on the EFdA-TP inhibition mechanism, we used a series of oligonucleotides that vary at positions upstream or downstream from the sites of EFdA-MP incorporation (Table 1). As a control we used ddATP, which always acts as a canonical ICT (data not shown).

With regard to the effect of changes before the site of EFdA-MP incorporation, remarkably we found that a single change in the template sequence can change the inhibition mechanism: the presence of C at a template position prior to the P6 site leads to exclusive ICT (Fig. 2A, T<sub>d31(5C)</sub>/P<sub>d18</sub>). In contrast, the presence of A, G, or T at the same template position leads primarily to DCT (Fig. 2A and Table 2; T<sub>d31(5A)</sub>/P<sub>d18</sub>, T<sub>d31(5G)</sub>/P<sub>d18</sub>, and T<sub>d31(5T)</sub>/P<sub>d18</sub>), although the presence of bands at the sites of EFdA incorporation (P6, P6, and P5, respectively) suggested an additional but less pronounced ICT mode of inhibition as well (none of these stopping patterns were observed in the absence of EFdA-TP).

Introducing a C before the incorporation site of EFdA-MP does not appear to always result in strong ICT. When we changed the P4 site of T<sub>d31(4G5T)</sub>/P<sub>d18</sub> to a C (T<sub>d31(4C5T)</sub>/P<sub>d18</sub>), we still observed a primarily DCT mode of inhibition (Fig. 2B), suggesting that sequences before and after the EFdA-MP incorporation site contribute to the preferred mechanism of inhibition.

EFdA-TP acted as an ICT at the P1 site regardless of the type of preceding nucleotide (Fig. 2A, gels in second column). To determine whether this strong preference is due to the upstream (P0) position being provided to the enzyme already in double-stranded DNA form (last primer nucleotide), we repeated the experiments using a shorter primer that stopped one position before the EFdA-MP incorporation site. The data shown in Fig. 2A, column 1, show that there was still ICT inhibition in all cases, whereas only in the case of T<sub>d31(0T)</sub>/P<sub>d17</sub> was there an apparent mixture of ICT and DCT.

We also tested the effect of template sequence at one position after the P6 or P1 site of EFdA-MP incorporation (P7 and P2

## Multiple Mechanisms of RT Inhibition by EFdA

sites in Fig. 2A, columns 4 and 3, respectively). We generally found no significant changes in the type of inhibition mechanism with the exception of  $T_{d31(2T)}/P_{d18}$ , which was now inhibited by both ICT and DCT instead of only ICT. Collectively, these results indicate that the mechanism of inhibition by EFdA can be influenced by the template sequence before and after the site of incorporation.

**TABLE 2**

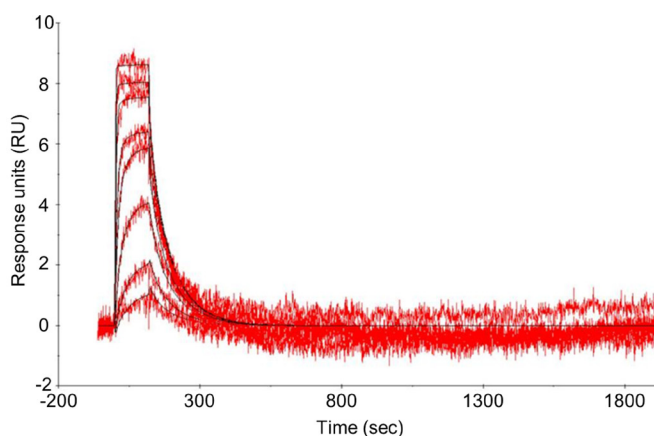
### Effect of template sequence on mechanism of action of EFdA-TP

The mechanism of inhibition by EFdA-TP was determined by the results in Fig. 2. Changes in the template sequences are indicated in bold.

T/P	Mechanism of action
<b>Effect of template sequence before EFdA-MP incorporation</b>	
$T_{d31(0A)}/P_{d17}$	P2: ICT
$T_{d31(0T)}/P_{d17}$	P1: ICT; P2: DCT/ICT
$T_{d31(0C)}/P_{d17}$	P2: ICT
$T_{d31(0G)}/P_{d17}$	P2: ICT
$T_{d31(0A)}/P_{d18}$	P1: ICT
$T_{d31(0T)}/P_{d18}$	P1: ICT
$T_{d31(0C)}/P_{d18}$	P1: ICT
$T_{d31(0G)}/P_{d18}$	P1: ICT
$T_{d31(5A)}/P_{d18}$	P6: ICT; P7: DCT
$T_{d31(5T)}/P_{d18}$	P5: ICT; P6: DCT/ICT
$T_{d31(4C5T)}/P_{d18}$	P5: ICT; P6: DCT/ICT
$T_{d31(5C)}/P_{d18}$	P6: ICT
$T_{d31(5G)}/P_{d18}$	P6: ICT; P7: DCT
<b>Effect of template sequence after EFdA-MP incorporation</b>	
$T_{d31(2A)}/P_{d18}$	P1: ICT
$T_{d31(2T)}/P_{d18}$	P1: ICT; P2: DCT/ICT
$T_{d31(2C)}/P_{d18}$	P1: ICT
$T_{d31(2G)}/P_{d18}$	P1: ICT
$T_{d31(7A)}/P_{d18}$	P6: ICT; P7: DCT
$T_{d31(7T)}/P_{d18}$	P6: ICT; P7: DCT/ICT
$T_{d31(7C)}/P_{d18}$	P6: ICT; P7: DCT
$T_{d31(7G)}/P_{d18}$	P6: ICT; P7: DCT

**EFdA-TP Binds RT Tighter than the Natural Substrate dATP**—Because EFdA-TP inhibits RT very efficiently, we wanted to examine and compare the binding affinity of the inhibitor and dATP with the enzyme. Therefore, we used SPR to determine the dissociation constant  $K_d$  for EFdA-TP and dATP. A two-state reaction protocol that assumes a 1:1 binding of substrate (EFdA-TP or dATP) to an immobilized ligand (RT) followed by a conformational change (“closing” of fingers subdomain) to form a stable complex (32–36) was used to analyze the SPR data. It is also assumed that a substrate in a complex that has undergone a conformational change can only dissociate if the conformational change is first reversed. This analysis generated the following kinetic values:  $k_{a1}$ , the association rate constant for substrate binding;  $k_{d1}$ , the dissociation rate constant for substrate from the complex;  $k_{a2}$ , the forward rate constant for the conformational change;  $k_{d2}$ , the reverse rate constant for the conformational change; and  $K_d$ , the overall equilibrium dissociation constant, which for this type of two-state reaction protocol is defined by  $(k_{d1}/k_{a1}) \cdot (k_{d2}/(k_{a2} + k_{d2}))$ . Fig. 3 shows that, using the  $T_{d20}/P_{d37}$ , the  $K_d$  for dATP is about 10 times higher than that of EFdA-TP. Hence, RT can bind EFdA-TP considerably more tightly than the natural substrate. This difference in the  $K_d$  of dATP and EFdA-TP is mostly due to an increased association rate for substrate binding ( $k_{a1}$ ) and increased forward rate constant for the conformational change ( $k_{a2}$ ) in the case of EFdA-TP (Fig. 3).

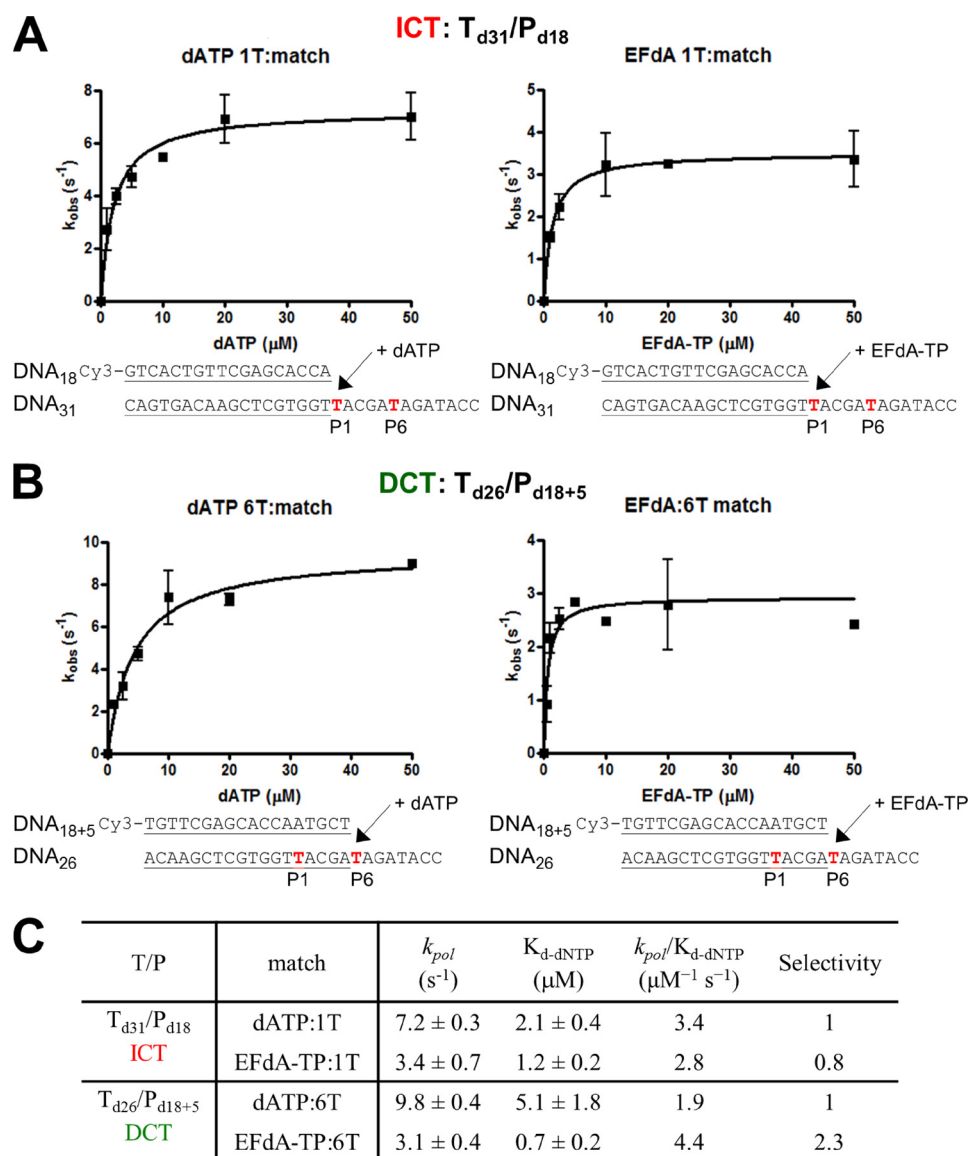
**RT Incorporates EFdA-TP Very Efficiently by Stalling Full Extension of the Terminated Primer**—To further understand the biochemical basis of the strong RT inhibition by EFdA-TP, we compared the incorporation efficiency of EFdA-TP with that of the natural substrate dATP under pre-steady state con-



Nucleotide	$K_{d,dNTP}$ / nM	$k_{a1}$ / $M^{-1}s^{-1}$	$k_{d1}$ / $s^{-1}$	$k_{a2}$ / $s^{-1}$	$k_{d2}$ / $s^{-1}$
EFdA-TP	18.6 (1)	$94.7 \cdot 10^4$ (1)	0.026 (1)	0.010 (1)	0.0224 (1)
dATP	192.8 (10.4)	$3.8 \cdot 10^4$ (0.04)	0.020 (0.8)	0.001 (0.1)	0.0006 (0.03)

**FIGURE 3. SPR to determine the kinetic constants of EFdA-TP and dATP binding to HIV-1 RT.** Nucleotide binding was performed by using RT covalently cross-linked to  $T_{d37}/P_{d20}$ , which has a 5'-biotinylated DNA template and a ddGMP incorporated at the primer. The RT-DNA<sub>ddGMP</sub> complex was immobilized on a streptavidin sensor chip, and increasing concentrations of dATP or EFdA-TP were flowed to allow nucleotide association and dissociation. A two-state reaction protocol was used to analyze the SPR data, which assume a 1:1 binding of substrate (EFdA-TP or dATP) to an immobilized ligand (RT) followed by a conformational change (closing of fingers subdomain) to form a stable complex. The graph shows the association and dissociation of EFdA-TP over time. This analysis generated the following kinetic values:  $k_{a1}$ , the association rate constant for substrate binding;  $k_{d1}$ , the dissociation rate constant for substrate from the complex;  $k_{a2}$ , the forward rate constant for the conformational change;  $k_{d2}$ , the reverse rate constant for the conformational change; and  $K_d$ , the overall equilibrium dissociation constant, which for this type of two-state reaction protocol is defined by  $K_d = (k_{d1}/k_{a1}) \cdot (k_{d2}/(k_{a2} + k_{d2}))$ . The -fold change of the various constants is shown in parentheses.





Values are determined from three independent experiments. Positions where EFdA-TP acts as an ICT or DCT are shown in red and green, respectively.

**FIGURE 4. Pre-steady state kinetics of correct single nucleotide incorporation of EFdA-TP and dATP by HIV-1 RT.** Preincubated HIV-1 RT (50 nM) and T<sub>d31</sub>/P<sub>d18</sub> (A) or T<sub>d26</sub>/P<sub>d18+5</sub> (50 nM) (B) were mixed by a quench-flow instrument with various concentrations of EFdA-TP or dATP for reaction times varying between 5 ms and 2 s. The amount of product at different reaction times was fit to the burst equation (Equation 1) to obtain burst phase rates of nucleotide incorporation. Observed rate constants were then plotted using a hyperbolic equation (Equation 3) to estimate  $k_{pol}$  and  $K_{d(dNTP)}$  (A and B). The sequences of the T/Ps are shown below the plots, and the calculated constants are shown in C. Error bars represent S.D. of at least two independent experiments.

ditions. Our results show that RT uses EFdA-TP very efficiently (Fig. 4). Interestingly, we demonstrated that depending on the sequence of the template the selectivity for EFdA-TP over the natural dATP substrate ranges from 0.8- to 2.3-fold. Another independent study using a different T/P showed that the incorporation efficiency of EFdA-TP is 2-fold higher than that of dATP (37). The high incorporation efficiency of EFdA-TP is mostly the result of the higher binding affinity of EFdA-TP (lower dissociation constant  $K_d$ ). These results are consistent with the SPR data that also showed an increased RT binding affinity for EFdA-TP compared with dATP using another T/P sequence.

Because EFdA-TP differs from the conventional chain terminators and possesses a 3'-OH group, we examined the possibil-

ity that there can be additional DNA polymerization events at the EFdA-MP end of T/P<sub>EFdA-MP</sub>. Primer extension experiments showed that when EFdA-TP acts as an ICT there is eventually slow full extension of the EFdA-MP-terminated primers (Fig. 5A). When EFdA-TP acts as a DCT, there is extension of the EFdA-MP primers by only one nucleotide under these conditions (Fig. 5B) and very little full extension over the course of hours (not shown). The extension of EFdA-MP-terminated primers has also been reported by Muftuoglu *et al.* (37) in the context of a different sequence and in the presence of higher dNTP and RT concentrations and is consistent with our findings reported here.

We used pre-steady state kinetics to quantify and compare the efficiencies of dNTP incorporation in EFdA-MP-termi-

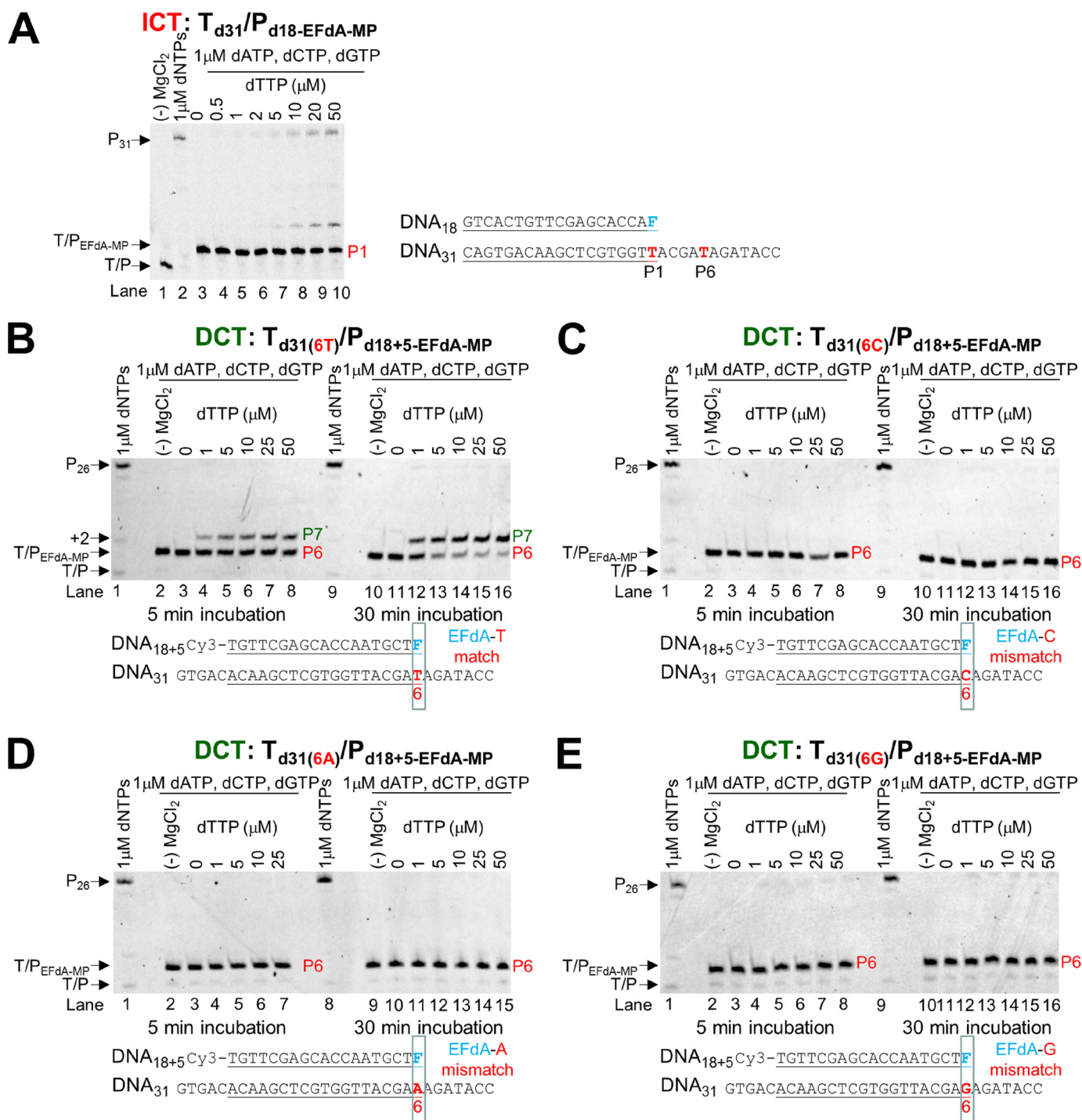


FIGURE 5. Incorporation of dNTPs into T/P<sub>EFdA-MP</sub> by HIV-1 RT. A, T<sub>d31</sub>/P<sub>d18-EFdA-MP</sub> (5 nM) was incubated with 20 nM HIV-1 RT, 6 mM MgCl<sub>2</sub>, 1  $\mu$ M dATP, dCTP, dGTP, and increasing concentrations of the next correct dNTP (dTTP, 0–50  $\mu$ M). The reactions were terminated after 15 min. B, T<sub>d31</sub>/P<sub>d18+5-EFdA-MP</sub> (5 nM) was incubated with 20 nM HIV-1 RT, 6 mM MgCl<sub>2</sub>, 1  $\mu$ M dATP, dCTP, dGTP, and increasing concentrations of the next correct dNTP (dTTP, 0–50  $\mu$ M). The reactions were terminated after 5 and 30 min. C–E, various T<sub>d31</sub>/P<sub>d18+5-EFdA-MP</sub> (5 nM) where EFdA-MP is incorporated as a mismatch were incubated with 20 nM HIV-1 RT, 6 mM MgCl<sub>2</sub>, 1  $\mu$ M dATP, dCTP, dGTP, and increasing concentrations of the next correct dNTP (dTTP, 0–50  $\mu$ M). The reactions were terminated after 5 and 30 min. The sequences of the T/Ps are shown below the gels, and the lanes are numbered for clarity.

ated primers at ICT (T<sub>d31</sub>/P<sub>d18-EFdA-MP</sub>) versus DCT (T<sub>d26</sub>/P<sub>d18+5-EFdA-MP</sub>) sites. Consistent with the gel-based results of Fig. 5, A and B, there was indeed a >400-fold difference in the extension efficiency of the EFdA-MP-terminated primers when different T/Ps were used (Table 3). Interestingly, when we simply changed a single template base from A to C at one position before the EFdA-MP incorporation site (Table 3), we

observed that the kinetics of dNTP incorporation on EFdA-MP-terminated primers were dramatically changed, showing a shift from a DCT to ICT mechanism. Using a single different T/P sequence, Muftuoglu *et al.* (37) recently showed that RT can incorporate dCTP after EFdA-MP 400 times more efficiently than it does after AMP (~1.5 versus 0.0034  $\mu$ M<sup>-1</sup>·s<sup>-1</sup>) (38).

**TABLE 3****Pre-steady state kinetic parameters of dTTP incorporation on T/P<sub>EFdA-MP</sub> by HIV-1 RT**

Values were determined from three independent experiments. Positions where EFdA-TP acts as an ICT or DCT are shown in red and green, respectively.

T/P	$k_{pol}$ ( $s^{-1} \times 10^{-3}$ )	$K_{d,dTTP}$ ( $\mu M$ )	$k_{pol}/K_{d,dTTP}$ ( $\mu M^{-1} s^{-1} \times 10^{-3}$ )	Fold difference
T <sub>d31</sub> /P <sub>d18</sub> -EFdA-MP <b>ICT</b>	1.8 ± 0.2	38.0 ± 7.3	0.05	1
T <sub>d26</sub> /P <sub>d18+5</sub> -EFdA-MP <b>DCT</b> (Template 5A)	7.6 ± 1.6	0.35 ± 0.1	22	440
T <sub>d26</sub> (5C)/P <sub>d18+5</sub> (5G)-EFdA-MP <b>ICT</b> (Template 5C)	4.6 ± 0.1	9.45 ± 3.2	0.5	10

**TABLE 4****Pre-steady state kinetic parameters of EFdA-TP and dATP match and mismatch incorporation by HIV-1 RT**

Values were determined from three independent experiments. Positions where EFdA-TP acts as an ICT or DCT are shown in red and green, respectively. The different templates vary in position X: G, C, or A.

T/P	match/mismatch	$k_{pol}$ ( $s^{-1} \times 10^{-3}$ )	$K_{d,dNTP}$ ( $\mu M$ )	$k_{pol}/K_{d,dNTP}$ ( $\mu M^{-1} s^{-1} \times 10^{-3}$ )
T <sub>d31</sub> (1X)/P <sub>d18</sub> <b>ICT</b>	EFdA-TP:1T	3,400 ± 700	1.2 ± 0.2	2,833
	EFdA-TP:1G	2.3 ± 0.1	0.8 ± 0.2	2.9
	EFdA-TP:1C	8.6 ± 1.6	8.5 ± 1.2	1.0
	EFdA-TP:1A	3.0 ± 0.5	1.5 ± 0.4	2.0
	dATP:1T	7,200 ± 300	2.1 ± 0.4	3,429
	dATP:1G	18.3 ± 2.0	28.0 ± 4.5	0.7
	dATP:1C	2.4 ± 0.5	1.8 ± 0.1	1.3
	dATP:1A	1.8 ± 1.3	66.0 ± 17.8	0.03
T <sub>d31</sub> (6X)/P <sub>d18+5</sub> <b>DCT</b>	EFdA-TP:6T	3,100 ± 400	0.7 ± 0.2	4,429
	EFdA-TP:6G	23.8 ± 4.0	9.2 ± 2.4	2.6
	EFdA-TP:6C	24.4 ± 1.9	17.2 ± 0.1	1.4
	EFdA-TP:6A	8.4 ± 1.3	9.7 ± 2.6	0.9
	dATP:6T	9,800 ± 400	5.1 ± 1.8	1,922
	dATP:6G	8.8 ± 1.1	2.8 ± 0.6	3.1
	dATP:6C	2.9 ± 0.1	3.6 ± 0.7	0.8
	dATP:6A	1.7 ± 0.5	19.8 ± 1.9	0.1

**EFdA-TP Is Efficiently Incorporated as a Mismatch but with No Further Extension**—The inhibition and incorporation experiments suggest that EFdA-TP can be used by RT as a substrate for DNA polymerization at levels even better than the natural dATP substrate. Using pre-steady state kinetics, we extended this finding by showing that EFdA-TP can be incorporated very efficiently not only as a cognate substrate but also as a mismatched substrate (Table 4). Specifically, EFdA-TP is incorporated as a mismatch more efficiently against a G than an A or a C. We also found that the template sequence affects the misincorporation efficiency in different ways for EFdA-TP and dATP. Hence, EFdA-MP is misincorporated more efficiently than dAMP at the P1 sites (ICT mechanism) when the mispairing base is opposite G or A, but not C (Table 4). In contrast, the misincorporation efficiencies of EFdA-MP and dAMP are similar at the P6 site (DCT mechanism) opposite G and C, whereas EFdA-MP is misincorporated more efficiently than dAMP opposite A. In addition, we tested the extension of primers terminated with misincorporated EFdA-MP (EFdA-MP opposite a C, A, or G) and found that there is no dNTP addition even at higher dNTP concentrations or incubation times (Fig. 5, C, D, and E) in contrast to the one-nucleotide extension of T/P<sub>EFdA-MP</sub> with EFdA-MP opposite the cognate base T (Fig. 5B).

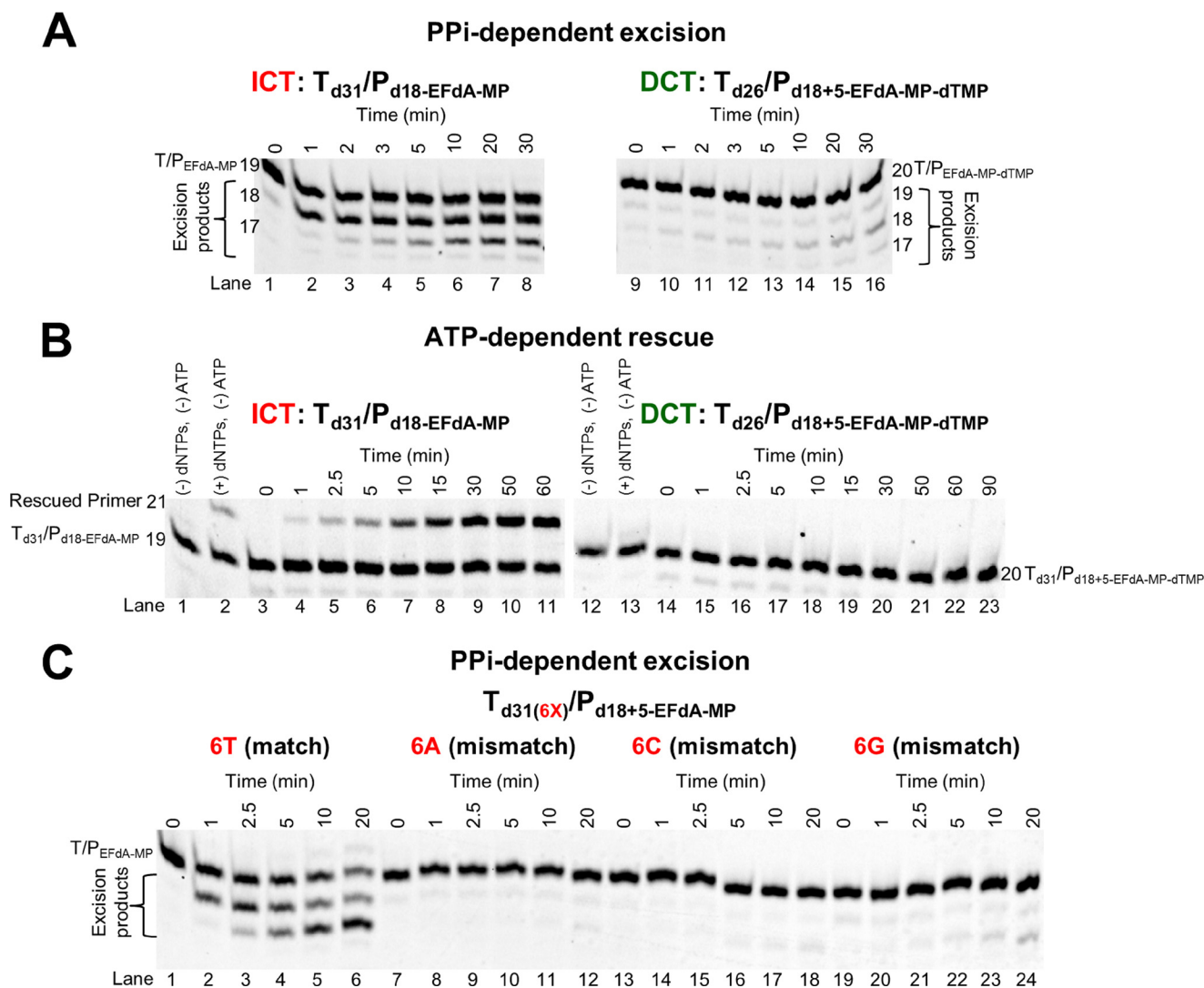
**Delayed Chain Termination Protects EFdA-MP from Excision**—One of the major mechanisms of resistance to NRTIs is the ATP-based excision of the chain terminator by RT (39, 40). The product of this excision reaction is a tetraphosphate

(NRTI-MP-ATP) and an unblocked primer that RT can use to resume DNA synthesis (41). For excision to occur, the NRTI-MP end of the chain-terminated primer should be positioned at the N-site (42). Our footprinting data in Fig. 1C establish that the translocation state, which reflects the position of RT on DNA, can be affected by the nucleic acid sequence. Specifically, in the absence of dNTP, T<sub>d43</sub>/P<sub>d30</sub>-EFdA is bound by RT in a pre-translocation mode (Fig. 1C, lane 7, left gel), whereas T<sub>d43</sub>/P<sub>d30+5</sub>-EFdA is bound in a post-translocation mode (Fig. 1C, lane 7, right gel). Importantly, these differences in binding lead to differences in the mechanism of EFdA inhibition with immediate chain termination at the site where translocation is not favored (P1 site of T<sub>d31</sub>/P<sub>d18</sub>) or delayed chain termination at the site where translocation is indeed favored (P6 site of T<sub>d31</sub>/P<sub>d18</sub>; Fig. 1, B and C). Because binding in a pre-translocation mode allows excision to occur (24, 28, 30), we hypothesized that the post-translocation bound T<sub>d26</sub>/P<sub>d18+5</sub>-EFdA-MP-dTMP would be protected from excision. To test this hypothesis, we performed ATP- or PP<sub>i</sub>-based phosphorolysis experiments to unblock the following EFdA-MP-terminated template primers: (a) T<sub>d31</sub>/P<sub>d18</sub>-EFdA-MP, which binds RT in a pre-translocation mode and is the product of ICT, and (b) T<sub>d26</sub>/P<sub>d18+5</sub>-EFdA-MP-dTMP, which binds RT in a post-translocation mode and is the product of DCT with a dTMP incorporated into the EFdA-MP-terminated primer.

We performed the experiments in the presence of either PP<sub>i</sub> or ATP. In the latter case, the excision reaction was coupled with the reverse DNA polymerization because dNTPs were also added in the reaction (rescue conditions). When EFdA-TP is inserted opposite P1 it acts as an ICT (as in T<sub>d31</sub>/P<sub>d18</sub>-EFdA-MP or T<sub>d43</sub>/P<sub>d18</sub>-EFdA-MP), and the nucleic acid is bound in a pre-translocation binding mode (Fig. 1C). In that case, there is some PP<sub>i</sub>-based excision of EFdA-MP from the 3'-end of the primer (Fig. 6A, left panel, lanes 2–8), although even in this case it does not appear to be a significant problem because there is facile reincorporation of EFdA-TP as we have shown previously (10). In addition, ATP-based rescue experiments showed that when a high concentration of competing dATP is included in the reaction we can detect rescue of the EFdA-MP-terminated primers (Fig. 6B, lanes 4–11) that are the ICT inhibition product, suggesting that when EFdA-MP is incorporated at an ICT site it is excised even though this phenomenon does not account for high level excision-based resistance as shown by our published virological data (11). In contrast, when EFdA-TP is inserted opposite P6, it acts as a DCT and allows a single incorporation event, which in the case of T<sub>d26</sub>/P<sub>d18+5</sub>-EFdA-MP-dTMP is a dTMP incorporation opposite P7. Under these conditions of DCT, there is a compelling suppression of PP<sub>i</sub>-based and ATP-based excision as shown in Fig. 6, right panels in A (lanes 10–16) and B (lanes 15–23). Hence, at sites of DCT, EFdA-MP-terminated primers are protected from excision, providing a strong advantage for EFdA-TP against excision-based resistance. Furthermore, mismatched primers that have EFdA-MP at the 3'-end are protected from excision (Fig. 6C, lanes 8–12, 14–18, and 20–24).

**EFdA-TP and TFV-DP Do Not Always Compete for the Same Incorporation Sites**—Because both EFdA and tenofovir are adenosine analogs, we wanted to see whether they would com-

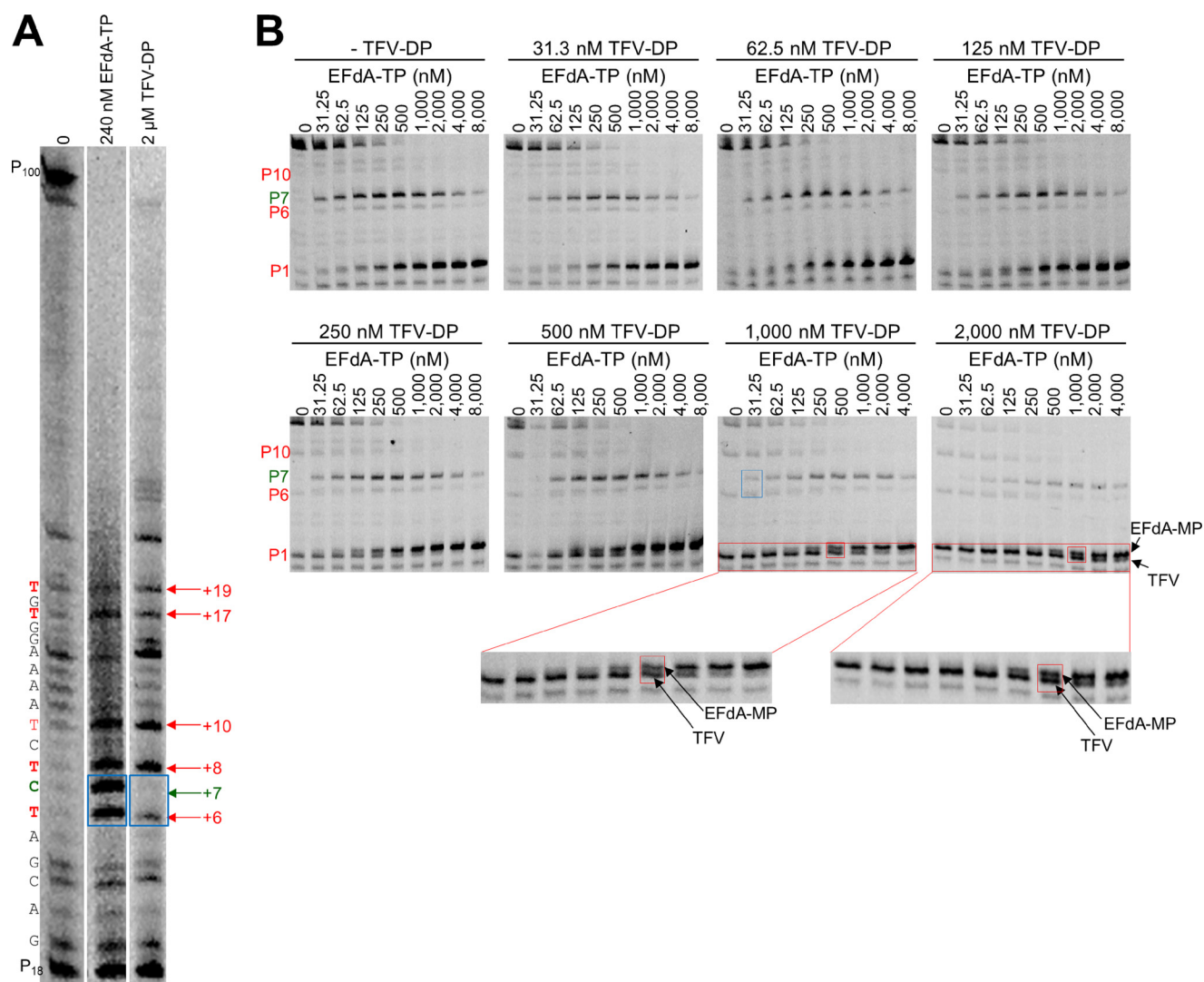




**FIGURE 6.  $PP_i$ - and ATP-dependent unblocking of EFdA-MP-terminated primers.** A, purified  $T_{d31}/P_{d18}\text{-EFdA-MP}$  or  $T_{d26}/P_{d18+5}\text{-EFdA-MP-dTMP}$  was incubated with HIV-1 RT in the presence of 6 mM  $MgCl_2$  and 150  $\mu M$   $PP_i$  at 37 °C. Aliquots were removed, and reactions were stopped at the indicated time points (0–30 min). The excision products are shown in braces. B, purified  $T_{d31}/P_{d18}\text{-EFdA-MP}$  or  $T_{d26}/P_{d18+5}\text{-EFdA-MP-dTMP}$  was incubated at 37 °C with HIV-1 RT in the presence of 10 mM  $MgCl_2$ , 3.5 mM ATP, and d(d)NTPs (100  $\mu M$  dATP, 0.5  $\mu M$  dTTP, and 10  $\mu M$  ddGTP for  $T_{d31}/P_{d18}\text{-EFdA-MP}$  or 100  $\mu M$  dTTP and 10  $\mu M$  ddCTP for  $T_{d26}/P_{d18+5}\text{-EFdA-MP-dTMP}$ ). Aliquots of the reactions were stopped at the indicated time points (0–90 min). C, purified  $T_{d31(6X)}/P_{d18+5}\text{-EFdA-MP}$  (where X = T, A, C, or G) was incubated with HIV-1 RT in the presence of 6 mM  $MgCl_2$  and 150  $\mu M$   $PP_i$  at 37 °C. Aliquots were removed, and reactions were stopped at the indicated time points (0–20 min). The excision products are shown in braces. The lane numbers are shown below each gel.

pete for the same incorporation sites. Surprisingly, when we used the active forms of the two analogs (EFdA-TP and TFV-DP) in parallel reactions at concentrations that resulted in approximately the same amount of primer extension (Fig. 7A, 2 versus lane 3), there were some differences in inhibitor incorporation as judged by stopping patterns. Specifically, although both inhibitors appeared to be incorporated opposite Ts (+6, +8, +10, +17, and +19) (Fig. 7A, lanes 2 and 3), there was a site that was strongly preferred by EFdA for DCT inhibition (+6 and +7 strong stops with no equivalent stops in the uninhibited first lane), whereas there was only moderate inhibition by TFV (weaker stop in the TFV-inhibited third lane). Furthermore, the +6 stop was weaker than the +10 stop for TFV but not for EFdA, providing initial evidence that the two adenosine analogs can have different incorporation efficiencies at different sites on the template. To further explore this possibility, we included both TFV-DP and EFdA-TP in the same reaction and in varying

ratios using a shorter  $T_{d31(7C)}/P_{d18}$  that allowed us to better resolve and monitor the EFdA-MP-terminated versus the TFV-terminated products. In each of the eight panels of Fig. 7B, we used increasing amounts of EFdA-TP in the presence of constant amounts of TFV-DP. Conveniently, we can follow incorporation of EFdA-MP and TFV in the same gels: hence, at the P1 site, the EFdA-MP-terminated primers ( $P_{d18}\text{-EFdA-MP}$ ) migrate slightly slower than the corresponding TFV-terminated primers ( $P_{d18}\text{-TFV}$ ) (Fig. 7B, red boxes). At the P6 site, we can compare TFV-based inhibition ( $P_{d18+5}\text{-TFV}$ ) with the EFdA-based inhibition ( $P_{d18+5}\text{-EFdA-MP-dTMP}$  at P7). We found that EFdA can compete with an excess of TFV more efficiently at the P6 versus at the P1 site: for example, in the presence of an excess of TFV (Fig. 7B, TFV = 1,000 nM), ~50% of chain termination at P6 is caused by ~31 nM EFdA (Fig. 7B, blue box), but the same ~50% chain termination at P1 is caused by ~500 nM EFdA (Fig. 7B, red box). Similar results can be seen at other



**FIGURE 7. EFdA-TP and TFV-DP have a different stopping pattern and do not always compete for the same incorporation sites.** A, using a long template,  $T_{d100r}$ , we investigated the stopping pattern of EFdA-TP and TFV-DP. At some positions, both analogs appear to have similar incorporation efficiency (same intensity of bands). However, at position +6, EFdA-MP is incorporated more efficiently than TFV, or TFV is not incorporated at all (+7; DCT site). The sequence of template is shown next to the gels. B,  $T_{d31(7C)}/P_{d18}$  (20 nM) was incubated with 20 nM RT for 15 min in the presence of 1  $\mu$ M dNTPs, 6 mM  $MgCl_2$ , and various concentrations of EFdA-TP and TFV-DP. The sites where the inhibitors act as ICT or DCT are shown in red and green, respectively. In red boxes, we highlight some examples of ICT where both analogs are equally incorporated. In the blue box, we highlight the ICT and DCT sites at P6 and P7, respectively, where TFV and EFdA-MP, respectively, are equally incorporated.

TFV concentrations in Fig. 7B. Collectively, these data suggest that EFdA-TP and TFV-DP have different inhibition site specificities.

## DISCUSSION

NRTIs were the first drugs used for the treatment of HIV infection and have always been part of first line antiretroviral therapies (1–8). All approved anti-HIV nucleoside analogs block RT-catalyzed DNA synthesis due to the lack of a 3'-OH group, which is necessary for DNA polymerization. Previously, we have shown that a series of 4'-substituted analogs with a 3'-OH possess anti-HIV activity (9–11). EFdA is the most potent of this series and, to our knowledge, the most potent NRTI with subnanomolar  $EC_{50}$  both in T-cells and peripheral blood mononuclear cells (10, 11, 16). The strong potency of EFdA is the result of its unique mechanism of action as well as its resistance to degradation by adenosine deaminase (15). Pre-

viously, we have reported that the inability of EFdA-MP-terminated primers to translocate from the N- to the P-site of HIV-1 RT causes inhibition of DNA polymerization (10). Here we demonstrate that EFdA inhibits RT with multiple mechanisms, which depend on the sequence of the nucleic acid substrate (Figs. 8 and 9).

There is a small number of reports on the effect of T/P sequence on RT inhibition by NRTIs. Scott and co-workers (43) reported that the primer terminus and adjacent upstream base pairs interact with HIV-1 RT in a sequence-dependent manner that affects the unblocking of NRTI-terminated primers. In addition, Hughes and co-workers (44) published that there is a difference in the extent of delayed chain termination by 4'-methyl dNTP analogs depending on the nucleic acid sequence. We report here that, depending on the T/P sequence, EFdA-TP can block RT either as a *de facto* ICT or as a DCT (Figs. 1, 2, 7, 8, and 9). Although EFdA-TP can inhibit RT both

## Multiple Mechanisms of RT Inhibition by EFdA

as an ICT and a DCT, it appears that it predominantly inhibits at the point of incorporation (four of five sites in Fig. 7A), causing immediate chain termination and preventing enzyme translocation (Figs. 1, 8, and 9), thus acting as a translocation-defective RT inhibitor (10). Nonetheless, we have identified sites at various template sequences where EFdA-TP can also act as a DCT; it does not block enzyme translocation, allowing the incorporation of one additional dNTP before DNA synthesis is terminated.

What factors may lead to the differences in the mechanism of EFdA inhibition at the P1 (ICT) and P6-P7 (ICT and DCT) sites? We initially examined the effect of inhibitor incorporation efficiency as we anticipated that at sites of efficient EFdA-MP incorporation the EFdA-MP-terminated primer products ( $T/P_{\text{EFdA-MP}}$ ) would be less likely to translocate, leading to immediate chain termination. Surprisingly, although EFdA-MP is better incorporated at the P6 site (Fig. 4), the footprinting experiments showed increased translocation at P6 (Fig. 1C), allowing more access to the dNTP-binding site and incorporation of the next complementary nucleotide ( $T/P_{\text{EFdA-MP-dNMP}}$ ). Further polymerization may be inhibited by unfavorable interactions between the 4'-ethynyl of  $T/P_{\text{EFdA-MP-dNMP}}$  and RT residues of the DNA-binding cleft.

We subsequently examined the effect of T/P sequence on the inhibition mechanism of EFdA. Our data definitively showed that a change of a single nucleotide can be sufficient to alter the inhibition mechanism from ICT to DCT (Fig. 2A,  $T_{\text{d31(5C)}}/P_{\text{d18}}$  versus  $T_{\text{d31(5A)}}/P_{\text{d18}}$ ), although in some cases, it does not have

an effect (Fig. 2B,  $T_{\text{d31(4G5T)}}/P_{\text{d18}}$  versus  $T_{\text{d31(4C5T)}}/P_{\text{d18}}$ ). Hence, we conclude that the T/P sequence is a major factor that can determine the inhibition mechanism of EFdA. Ongoing structural studies are designed to determine the molecular basis for this specificity.

The ability of EFdA to inhibit RT with multiple mechanisms may have implications for current anti-HIV therapies. We recently showed that the combination of EFdA and TFV had an effect on the inhibition of HIV replication in cell culture (16). This was an unexpected finding as both NRTIs are analogs of dA. A partial explanation is provided in the present study where we show examples of template sites where TFV is not incorporated efficiently (Fig. 7A, lane 3, faint band at template position +6), whereas EFdA-MP very efficiently blocked RT with both ICT and DCT mechanisms (Fig. 7A, lane 2, strong bands at template positions +6 and +7). Differences in the mechanism of activation to their respective active forms may partially be responsible for the lack of competition between EFdA and TFV (16).

Although  $T/P_{\text{EFdA-MP}}$  is generally ideally located to undergo phosphorolytic excision, with EFdA-MP positioned at the N-site (Fig. 8) (24, 30, 39), excision-based resistance is not a major pathway for resistance to EFdA (11).<sup>5</sup> This is likely because of the apparently high reincorporation efficiency of the newly excised EFdA-TP. Furthermore, as shown in Fig. 6, when EFdA-MP is incorporated as a DCT,  $T/P_{\text{EFdA-MP-dTMP}}$  is protected from excision, resulting in decreased drug resistance by the excision mechanism. Moreover, we did not observe excision of EFdA-MP-terminated primers in positions where EFdA-MP is incorporated as a mismatch (Fig. 6C). These data are consistent with our earlier cell-based data demonstrating that EFdA maintains its potency against HIV strains that carry excision-based zidovudine resistance mutations (11).

There are two nucleos(t)ide analog drugs that retain a 3'-OH and have been approved for the treatment of viral infections: entecavir, which is the most potent anti-hepatitis B virus nucleoside analog drug (45, 46), and sofosbuvir, which is a recently approved anti-hepatitis C virus nucleotide analog drug (47, 48). So far, there are no NRTIs with a 3'-OH group that are approved for the treatment of HIV infections. EFdA could be paired with approved anti-HIV drugs, leading to synergistic and

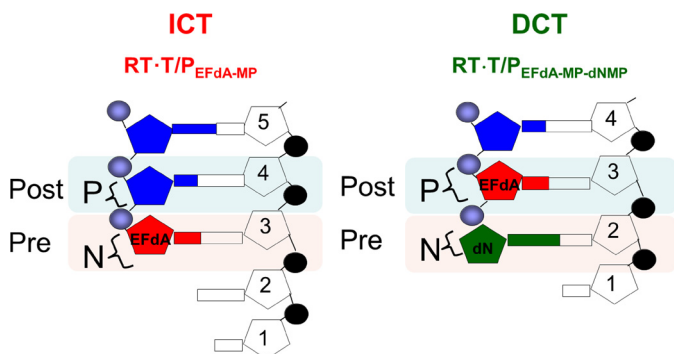

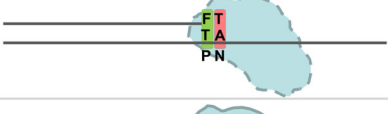



FIGURE 8. **Schematic representation of EFdA-MP-containing complexes.** EFdA acts as an ICT by occupying the N-site of RT, whereas it occupies the P-site of RT when it acts as a DCT. In this case, the N-site is free for the next incoming dNMP to be incorporated.

<sup>5</sup> B. Marchand, X. Tu, K. Kirby, E. Michailidis, O. Ihenacho, E. Kodama, H. Mitsuya, M. Parniak, and S. Sarafianos, unpublished data.

Mechanism of inhibition	Effect	Schematic representation
<b>ICT (immediate chain termination)</b> Blocks DNA synthesis at the point of EFdA-MP incorporation	Translocation is blocked and kinetics are dramatically slowed down	
<b>DCT (delayed chain termination)</b> EFdA-MP-terminated primers are extended by one nucleotide before DNA synthesis is blocked	RT falls off or is misaligned on the T/P and DNA synthesis is blocked. EFdA-MP-terminated primers are protected from excision.	
<b>EFdA misincorporation</b> EFdA-MP is efficiently incorporated as a mismatch	Primers with EFdA-MP at the 3'-end as a mismatch are not fully-extended and cannot be unblocked by RT	

Nucleic acid substrate sequence: nucleotides before and after EFdA-MP incorporation affect mechanism of inhibition

FIGURE 9. **Overview of the multiple mechanisms of RT inhibition by EFdA.**



additive effects as shown in cell-based assays, and it also suppressed viral loads in macaques to undetectable levels within a week of treatment and without any signs of toxicity (9, 11, 16, 17, 44). Its ability to inhibit RT by multiple mechanisms imparts excellent antiviral activity (11) and may contribute to its favorable resistance profile (49), thus rendering it a potentially promising new generation NRTI.

## REFERENCES

1. Hammer, S. M., Saag, M. S., Schechter, M., Montaner, J. S., Schooley, R. T., Jacobsen, D. M., Thompson, M. A., Carpenter, C. C., Fischl, M. A., Gazzard, B. G., Gatell, J. M., Hirsch, M. S., Katzenstein, D. A., Richman, D. D., Vella, S., Yeni, P. G., and Volberding, P. A. (2006) Treatment for adult HIV infection: 2006 recommendations of the International AIDS Society–U.S.A. panel. *Top. HIV Med.* **14**, 827–843
2. Schinazi, R. F., Hernandez-Santiago, B. I., and Hurwitz, S. J. (2006) Pharmacology of current and promising nucleosides for the treatment of human immunodeficiency viruses. *Antiviral Res.* **71**, 322–334
3. Parniak, M. A., and Sluis-Cremer, N. (2000) Inhibitors of HIV-1 reverse transcriptase. *Adv. Pharmacol.* **49**, 67–109
4. De Clercq, E. (2007) Anti-HIV drugs. *Verh. K. Acad. Geneesk. Belg.* **69**, 81–104
5. Sluis-Cremer, N., and Tachedjian, G. (2008) Mechanisms of inhibition of HIV replication by non-nucleoside reverse transcriptase inhibitors. *Virus Res.* **134**, 147–156
6. Deval, J. (2009) Antimicrobial strategies: inhibition of viral polymerases by 3'-hydroxyl nucleosides. *Drugs* **69**, 151–166
7. Sharma, P. L., Nurpeisov, V., Hernandez-Santiago, B., Beltran, T., and Schinazi, R. F. (2004) Nucleoside inhibitors of human immunodeficiency virus type 1 reverse transcriptase. *Curr. Top. Med. Chem.* **4**, 895–919
8. Sarafianos, S. G., Marchand, B., Das, K., Himmel, D. M., Parniak, M. A., Hughes, S. H., and Arnold, E. (2009) Structure and function of HIV-1 reverse transcriptase: molecular mechanisms of polymerization and inhibition. *J. Mol. Biol.* **385**, 693–713
9. Kodama, E. I., Kohgo, S., Kitano, K., Machida, H., Gatanaga, H., Shigeta, S., Matsuoka, M., Ohnishi, K., and Mitsuya, H. (2001) 4'-Ethynyl nucleoside analogs: potent inhibitors of multidrug-resistant human immunodeficiency virus variants *in vitro*. *Antimicrob. Agents Chemother.* **45**, 1539–1546
10. Michailidis, E., Marchand, B., Kodama, E. N., Singh, K., Matsuoka, M., Kirby, K. A., Ryan, E. M., Sawani, A. M., Nagy, E., Ashida, N., Mitsuya, H., Parniak, M. A., and Sarafianos, S. G. (2009) Mechanism of inhibition of HIV-1 reverse transcriptase by 4'-ethynyl-2-fluoro-2'-deoxyadenosine triphosphate, a translocation-defective reverse transcriptase inhibitor. *J. Biol. Chem.* **284**, 35681–35691
11. Kawamoto, A., Kodama, E., Sarafianos, S. G., Sakagami, Y., Kohgo, S., Kitano, K., Ashida, N., Iwai, Y., Hayakawa, H., Nakata, H., Mitsuya, H., Arnold, E., and Matsuoka, M. (2008) 2'-Deoxy-4'-C-ethynyl-2-halo-adenosines active against drug-resistant human immunodeficiency virus type 1 variants. *Int. J. Biochem. Cell Biol.* **40**, 2410–2420
12. Ohnishi, H. (2006) 2'-Deoxy-4'-C-ethynyl-2-fluoroadenosine, a nucleoside reverse transcriptase inhibitor, is highly potent against all human immunodeficiency viruses type 1 and has low toxicity. *Chem. Rec.* **6**, 133–143
13. Kageyama, M., Nagasawa, T., Yoshida, M., Ohnishi, H., and Kuwahara, S. (2011) Enantioselective total synthesis of the potent anti-HIV nucleoside EFdA. *Org. Lett.* **13**, 5264–5266
14. Gallois-Montbrun, S., Schneider, B., Chen, Y., Giacomoni-Fernandes, V., Mulard, L., Morera, S., Janin, J., Deville-Bonne, D., and Veron, M. (2002) Improving nucleoside diphosphate kinase for antiviral nucleotide analogs activation. *J. Biol. Chem.* **277**, 39953–39959
15. Kirby, K. A., Michailidis, E., Fetterly, T. L., Steinbach, M. A., Singh, K., Marchand, B., Leslie, M. D., Hagedorn, A. N., Kodama, E. N., Marquez, V. E., Hughes, S. H., Mitsuya, H., Parniak, M. A., and Sarafianos, S. G. (2013) Effects of 4'- and 2-substitutions on the bioactivity of 4'-ethynyl-2-fluoro-2'-deoxyadenosine. *Antimicrob. Agents Chemother.* **57**, 6254–6264
16. Hachiya, A., Reeve, A. B., Marchand, B., Michailidis, E., Ong, Y. T., Kirby, K. A., Leslie, M. D., Oka, S., Kodama, E. N., Rohan, L. C., Mitsuya, H., Parniak, M. A., and Sarafianos, S. G. (2013) Evaluation of combinations of 4'-ethynyl-2-fluoro-2'-deoxyadenosine with clinically used antiretroviral drugs. *Antimicrob. Agents Chemother.* **57**, 4554–4558
17. Murphey-Corb, M., Rajakumar, P., Michael, H., Nyaundi, J., Didier, P. J., Reeve, A. B., Mitsuya, H., Sarafianos, S. G., and Parniak, M. A. (2012) Response of simian immunodeficiency virus to the novel nucleoside reverse transcriptase inhibitor 4'-ethynyl-2-fluoro-2'-deoxyadenosine *in vitro* and *in vivo*. *Antimicrob. Agents Chemother.* **56**, 4707–4712
18. Bauman, J. D., Das, K., Ho, W. C., Baweja, M., Himmel, D. M., Clark, A. D., Jr., Oren, D. A., Boyer, P. L., Hughes, S. H., Shatkin, A. J., and Arnold, E. (2008) Crystal engineering of HIV-1 reverse transcriptase for structure-based drug design. *Nucleic Acids Res.* **36**, 5083–5092
19. Schuckmann, M. M., Marchand, B., Hachiya, A., Kodama, E. N., Kirby, K. A., Singh, K., and Sarafianos, S. G. (2010) The N348I mutation at the connection subdomain of HIV-1 reverse transcriptase decreases binding to nevirapine. *J. Biol. Chem.* **285**, 38700–38709
20. Ndongwe, T. P., Adediji, A. O., Michailidis, E., Ong, Y. T., Hachiya, A., Marchand, B., Ryan, E. M., Rai, D. K., Kirby, K. A., Whatley, A. S., Burke, D. H., Johnson, M., Ding, S., Zheng, Y. M., Liu, S. L., Kodama, E., Delviks-Frankenberry, K. A., Pathak, V. K., Mitsuya, H., Parniak, M. A., Singh, K., and Sarafianos, S. G. (2012) Biochemical, inhibition and inhibitor resistance studies of xenotropic murine leukemia virus-related virus reverse transcriptase. *Nucleic Acids Res.* **40**, 345–359
21. Kirby, K. A., Marchand, B., Ong, Y. T., Ndongwe, T. P., Hachiya, A., Michailidis, E., Leslie, M. D., Sietsema, D. V., Fetterly, T. L., Dorst, C. A., Singh, K., Wang, Z., Parniak, M. A., and Sarafianos, S. G. (2012) Structural and inhibition studies of the RNase H function of xenotropic murine leukemia virus-related virus reverse transcriptase. *Antimicrob. Agents Chemother.* **56**, 2048–2061
22. Michailidis, E., Ryan, E. M., Hachiya, A., Kirby, K. A., Marchand, B., Leslie, M. D., Huber, A. D., Ong, Y. T., Jackson, J. C., Singh, K., Kodama, E. N., Mitsuya, H., Parniak, M. A., and Sarafianos, S. G. (2013) Hypersusceptibility mechanism of tenofovir-resistant HIV to EFdA. *Retrovirology* **10**, 65
23. Michailidis, E., Singh, K., Ryan, E. M., Hachiya, A., Ong, Y. T., Kirby, K. A., Marchand, B., Kodama, E. N., Mitsuya, H., Parniak, M. A., and Sarafianos, S. G. (2012) Effect of translocation defective reverse transcriptase inhibitors on the activity of N348I, a connection subdomain drug resistant HIV-1 reverse transcriptase mutant. *Cell. Mol. Biol.* **58**, 187–195
24. Sarafianos, S. G., Clark, A. D., Jr., Tuske, S., Squire, C. J., Das, K., Sheng, D., Ilankumaran, P., Ramesha, A. R., Kroth, H., Sayer, J. M., Jerina, D. M., Boyer, P. L., Hughes, S. H., and Arnold, E. (2003) Trapping HIV-1 reverse transcriptase before and after translocation on DNA. *J. Biol. Chem.* **278**, 16280–16288
25. Meyer, P. R., Matsuura, S. E., So, A. G., and Scott, W. A. (1998) Unblocking of chain-terminated primer by HIV-1 reverse transcriptase through a nucleotide-dependent mechanism. *Proc. Natl. Acad. Sci. U.S.A.* **95**, 13471–13476
26. Singh, K., Marchand, B., Rai, D. K., Sharma, B., Michailidis, E., Ryan, E. M., Matzek, K. B., Leslie, M. D., Hagedorn, A. N., Li, Z., Norden, P. R., Hachiya, A., Parniak, M. A., Xu, H. T., Wainberg, M. A., and Sarafianos, S. G. (2012) Biochemical mechanism of HIV-1 resistance to rilpivirine. *J. Biol. Chem.* **45**, 38110–38123
27. Johnson, K. A. (1993) Conformational coupling in DNA polymerase fidelity. *Annu. Rev. Biochem.* **62**, 685–713
28. Sarafianos, S. G., Clark, A. D., Jr., Das, K., Tuske, S., Birktoft, J. J., Ilankumaran, P., Ramesha, A. R., Sayer, J. M., Jerina, D. M., Boyer, P. L., Hughes, S. H., and Arnold, E. (2002) Structures of HIV-1 reverse transcriptase with pre- and post-translocation AZTMP-terminated DNA. *EMBO J.* **21**, 6614–6624
29. Hachiya, A., Kodama, E. N., Schuckmann, M. M., Kirby, K. A., Michailidis, E., Sakagami, Y., Oka, S., Singh, K., and Sarafianos, S. G. (2011) K70Q adds high-level tenofovir resistance to "Q151M complex" HIV reverse transcriptase through the enhanced discrimination mechanism. *PLoS One* **6**, e16242
30. Marchand, B., and Gotte, M. (2003) Site-specific footprinting reveals differences in the translocation status of HIV-1 reverse transcriptase. Implications for polymerase translocation and drug resistance. *J. Biol. Chem.*

- 278, 35362–35372
31. Biaglow, J. E., and Kachur, A. V. (1997) The generation of hydroxyl radicals in the reaction of molecular oxygen with polyphosphate complexes of ferrous ion. *Radiat. Res.* **148**, 181–187
32. Hu, W. S., and Hughes, S. H. (2012) HIV-1 reverse transcription. *Cold Spring Harb. Perspect. Med.* **2**, a006882
33. Huang, H., Chopra, R., Verdine, G. L., and Harrison, S. C. (1998) Structure of a covalently trapped catalytic complex of HIV-1 reverse transcriptase: implications for drug resistance. *Science* **282**, 1669–1675
34. Tuske, S., Sarafianos, S. G., Clark, A. D., Jr., Ding, J., Naeger, L. K., White, K. L., Miller, M. D., Gibbs, C. S., Boyer, P. L., Clark, P., Wang, G., Gaffney, B. L., Jones, R. A., Jerina, D. M., Hughes, S. H., and Arnold, E. (2004) Structures of HIV-1 RT-DNA complexes before and after incorporation of the anti-AIDS drug tenofovir. *Nat. Struct. Mol. Biol.* **11**, 469–474
35. Das, K., Bandwar, R. P., White, K. L., Feng, J. Y., Sarafianos, S. G., Tuske, S., Tu, X., Clark, A. D., Jr., Boyer, P. L., Hou, X., Gaffney, B. L., Jones, R. A., Miller, M. D., Hughes, S. H., and Arnold, E. (2009) Structural basis for the role of the K65R mutation in HIV-1 reverse transcriptase polymerization, excision antagonism, and tenofovir resistance. *J. Biol. Chem.* **284**, 35092–35100
36. Lansdon, E. B., Samuel, D., Lagpacan, L., Brendza, K. M., White, K. L., Hung, M., Liu, X., Boojamra, C. G., Mackman, R. L., Cihlar, T., Ray, A. S., McGrath, M. E., and Swaminathan, S. (2010) Visualizing the molecular interactions of a nucleotide analog, GS-9148, with HIV-1 reverse transcriptase-DNA complex. *J. Mol. Biol.* **397**, 967–978
37. Muftuoglu, Y., Sohl, C. D., Mislak, A. C., Mitsuya, H., Sarafianos, S. G., and Anderson, K. S. (2014) Probing the molecular mechanism of action of the HIV-1 reverse transcriptase inhibitor 4'-ethynyl-2-fluoro-2'-deoxyadenosine (EFdA) using pre-steady-state kinetics. *Antiviral Res.* **106**, 1–4
38. Kim, J., Roberts, A., Yuan, H., Xiong, Y., and Anderson, K. S. (2012) Nucleocapsid protein annealing of a primer-template enhances (+)-strand DNA synthesis and fidelity by HIV-1 reverse transcriptase. *J. Mol. Biol.* **415**, 866–880
39. Arion, D., Kaushik, N., McCormick, S., Borkow, G., and Parniak, M. A. (1998) Phenotypic mechanism of HIV-1 resistance to 3'-azido-3'-deoxythymidine (AZT): increased polymerization processivity and enhanced sensitivity to pyrophosphate of the mutant viral reverse transcriptase. *Biochemistry* **37**, 15908–15917
40. Meyer, P. R., Matsuura, S. E., Mian, A. M., So, A. G., and Scott, W. A. (1999) A mechanism of AZT resistance: an increase in nucleotide-dependent primer unblocking by mutant HIV-1 reverse transcriptase. *Mol. Cell* **4**, 35–43
41. Sarafianos, S. G., Hughes, S. H., and Arnold, E. (2004) Designing anti-AIDS drugs targeting the major mechanism of HIV-1 RT resistance to nucleoside analog drugs. *Int. J. Biochem. Cell Biol.* **36**, 1706–1715
42. Boyer, P. L., Sarafianos, S. G., Arnold, E., and Hughes, S. H. (2001) Selective excision of AZTMP by drug-resistant human immunodeficiency virus reverse transcriptase. *J. Virol.* **75**, 4832–4842
43. Meyer, P. R., Smith, A. J., Matsuura, S. E., and Scott, W. A. (2004) Effects of primer-template sequence on ATP-dependent removal of chain-terminating nucleotide analogues by HIV-1 reverse transcriptase. *J. Biol. Chem.* **279**, 45389–45398
44. Vu, B. C., Boyer, P. L., Siddiqui, M. A., Marquez, V. E., and Hughes, S. H. (2011) 4'-C-Methyl-2'-deoxyadenosine and 4'-C-ethyl-2'-deoxyadenosine inhibit HIV-1 replication. *Antimicrob. Agents Chemother.* **55**, 2379–2389
45. Woo, G., Tomlinson, G., Nishikawa, Y., Kowgier, M., Sherman, M., Wong, D. K., Pham, B., Ungar, W. J., Einarson, T. R., Heathcote, E. J., and Krahn, M. (2010) Tenofovir and entecavir are the most effective antiviral agents for chronic hepatitis B: a systematic review and Bayesian meta-analyses. *Gastroenterology* **139**, 1218–1229
46. Michailidis, E., Kirby, K. A., Hachiya, A., Yoo, W., Hong, S. P., Kim, S. O., Folk, W. R., and Sarafianos, S. G. (2012) Antiviral therapies: focus on hepatitis B reverse transcriptase. *Int. J. Biochem. Cell Biol.* **44**, 1060–1071
47. Lawitz, E., Mangia, A., Wyles, D., Rodriguez-Torres, M., Hassanein, T., Gordon, S. C., Schultz, M., Davis, M. N., Kayali, Z., Reddy, K. R., Jacobson, I. M., Kowdley, K. V., Nyberg, L., Subramanian, G. M., Hyland, R. H., Arterburn, S., Jiang, D., McNally, J., Brainard, D., Symonds, W. T., McHutchison, J. G., Sheikh, A. M., Younossi, Z., and Gane, E. J. (2013) Sofosbuvir for previously untreated chronic hepatitis C infection. *N. Engl. J. Med.* **368**, 1878–1887
48. Gentile, I., Borgia, F., Buonomo, A. R., Castaldo, G., and Borgia, G. (2013) A novel promising therapeutic option against hepatitis C virus: an oral nucleotide NS5B polymerase inhibitor sofosbuvir. *Curr. Med. Chem.* **20**, 3733–3742
49. Maeda, K., Desai, D. V., Aoki, M., Nakata, H., Kodama, E. N., and Mitsuya, H. (2014) Delayed emergence of HIV-1 variants resistant to 4'-ethynyl-2-fluoro-2'-deoxyadenosine: comparative sequential passage study with lamivudine, tenofovir, emtricitabine and BMS-986001. *Antiviral Ther.* **19**, 179–189